ACTA GEOLOGICAHISPANICA, v. 36 (2001), nº 3-4, p. 329-354

Paleoseismic results from multiple trenching analysis along a silent fault: The El Camp fault (Tarragona, northeastern Iberian Peninsula)

Resultados paleosísmicos obtenidos del análisis de trincheras en una falla silenciosa: la falla de El Camp (Tarragona, nordeste de la Península Ibérica)

E. MASANA, J.A. VILLAMARÍN and P. SANTANACH

Departament de Geologia Dinàmica i Geofísica, Universitat de Barcelona, Zona Universitària de Pedralbes, 08028 Barcelona. eula@natura.geo.ub.es

ABSTRACT

We present the paleoseismological analysis of the El Camp fault scarp. Paleoseismology constitutes the key methodology for any real estimate of seismic hazard in low-slip-rate areas with no reported historical earthquakes. The recent tectonic activity of this fault is evidenced by a young mountain front and a fault scarp which cuts Quaternary alluvial fans. A regional geological analysis indicates that three generations of alluvial fans are cut by the fault. Absolute (TL and U/Th) and relative datings show that the oldest fan is 300 ka old and the intermediate one is 125 ka old. The study of 7 trenches and the absolute datings performed (TL, U/Th, radiocarbon as well as pollen analysis) revealed the following: 1) the El Camp fault consists of two segments (the northern end of the southern segment is located close to Porquerola creek); 2) only the southern segment has been active since 125 ka; 3) the fault is seismogenic because it is associated with liquefaction features and colluvial wedges; 4) the El Camp fault has produced at least three well constrained surface-rupturing earthquakes since 125 ka (events Z, Y, and X). Based on the different tectonic features observed in the trenches, the recurrence period of large earthquakes during this period was estimated to be around 30 ka and the elapsed time to be around 3000 yr. Using the fault length and the vertical displacement per event, the largest estimated earthquake had a magnitude of M_W 6.7.

Keywords: Paleoseismicity. Trenching. Normal fault. Alluvial fans. Catalan Coastal Ranges.

RESUMEN

Se presenta el análisis paleosismológico de la falla de El Camp. La paleosismología es una herramienta imprescindible para la caracterización sísmica de fallas activas, lentas y sin sismicidad histórica y, por lo tanto, para cálculos de peligrosidad sísmica. La falla de

El Camp muestra evidencias de actividad tectónica: un frente montañoso joven y un escarpe de falla que afecta a abanicos aluviales cuaternarios. Un análisis geológico regional, previo al paleosismológico, muestra tres generaciones de abanicos aluviales afectados por la falla. El techo de éstos ha sido datado (U/Th y TL en caliches) en 300 y 125 ka para las dos generaciones más antiguas. Del estudio de 7 trincheras y de las dataciones por U/Th, TL, radiocarbono y polen se han obtenido los siguientes resultados: 1) La falla tiene dos segmentos con límite en el barranco de la Porquerola. Solamente el segmento al sur de este punto ha sido activo posteriormente a 125 ka. 2) La falla de El Camp es sismogénica. 3) Se han caracterizado un mínimo de tres eventos posteriores a 125 ka (eventos Z, Y, y X). 4) El período intersísmico reciente se ha estimado en 30 ka. 5) El tiempo transcurrido desde el último terremoto es de 3000 años. 6) La magnitud del terremoto máximo es M_W 6.7.

Palabras clave: Paleosismicidad. Trincheras. Falla normal. Abanicos aluviales. Cadenas Costeras Catalanas.

INTRODUCTION

One of the aims of paleoseismology is to characterize the seismic and related faulting behavior of a zone in order to better constrain its seismic hazard. The seismic hazard of a region can be defined as the probability of exceedence of a given value of ground acceleration (or intensity, magnitude, velocity...) during a certain period of time. Thus, an adequate seismic hazard analysis requires a sound knowledge of the seismic behavior of the studied area, which involves at least knowledge of one entire seismic cycle. It is, therefore, of considerable interest to constrain the duration of this cycle, which depends on the tectonic context of the area. The seismic cycle may vary, for example, from 10^2 yr along active plate boundaries to 10^6 yr in stable continents (Giardini, 1995). Seismic hazard analysis has been developed in areas where society is affected by high seismic activity. Areas with high seismicity are, in most cases, situated along active faults with high slip-rates, i.e. along active plate boundaries or related structures. In such cases, the seismic cycle is short and seismic hazard analysis based on a complete and sufficiently long historical seismic catalog is adequate. On the other hand, seismic hazard evaluation is problematic in areas without a historical seismic catalog or with a short catalog, and low slip rates. Paleoseismology has become an essential tool in this regard since it provides the necessary seismic parameters of the seismogenic slow faults. A number of studies based on paleoseismological data have characterized the activity of different faults such as the Wasatch fault (Machette et al., 1992), the San Andreas fault (Sieh, 1978), in the West of the United States, and the Roer Graben fault in Europe (Camelbeeck and Meghraoui, 1998).

Figure 1. Seismicity map of the Iberian Peninsula. Squares indicate historical seismicity and dots represent instrumentally registered events. Note that there is no seismicity in the surroundings of the El Camp fault. Data from Instituto Geográfico Nacional (IGN).

Figura 1. Mapa de la sismicidad de la Península Ibérica. Los cuadrados indican la sismicidad histórica y los puntos los eventos registrados instrumentalmente. Nótese la ausencia de sismicidad en los alrededores de la falla de El Camp. Datos del Instituto Geográfico Nacional (IGN).

The level of seismic hazard in the Iberian Peninsula has been considered to be low because of the infrequency of catastrophic earthquakes in the historical catalog (Fig. 1). Nevertheless, two arguments challenge this assumption: 1) the incompleteness of the catalog within the period covered and, 2) the difference between the period covered by the catalog (not longer than 700 yr) and the duration of the seismic cycle (which in this particular tectonic framework can vary between 10^3 yr and 10^5 yr according to Giardini, 1995). Paleoseismology can help to resolve some of these problems by identifying and characterizing large pre-historical earthquakes. This is of considerable importance in the Iberian Peninsula, where many active faults have low slip rates. It is even of greater importance along the El Camp fault where the lack of historical seismicity could lead to erroneous

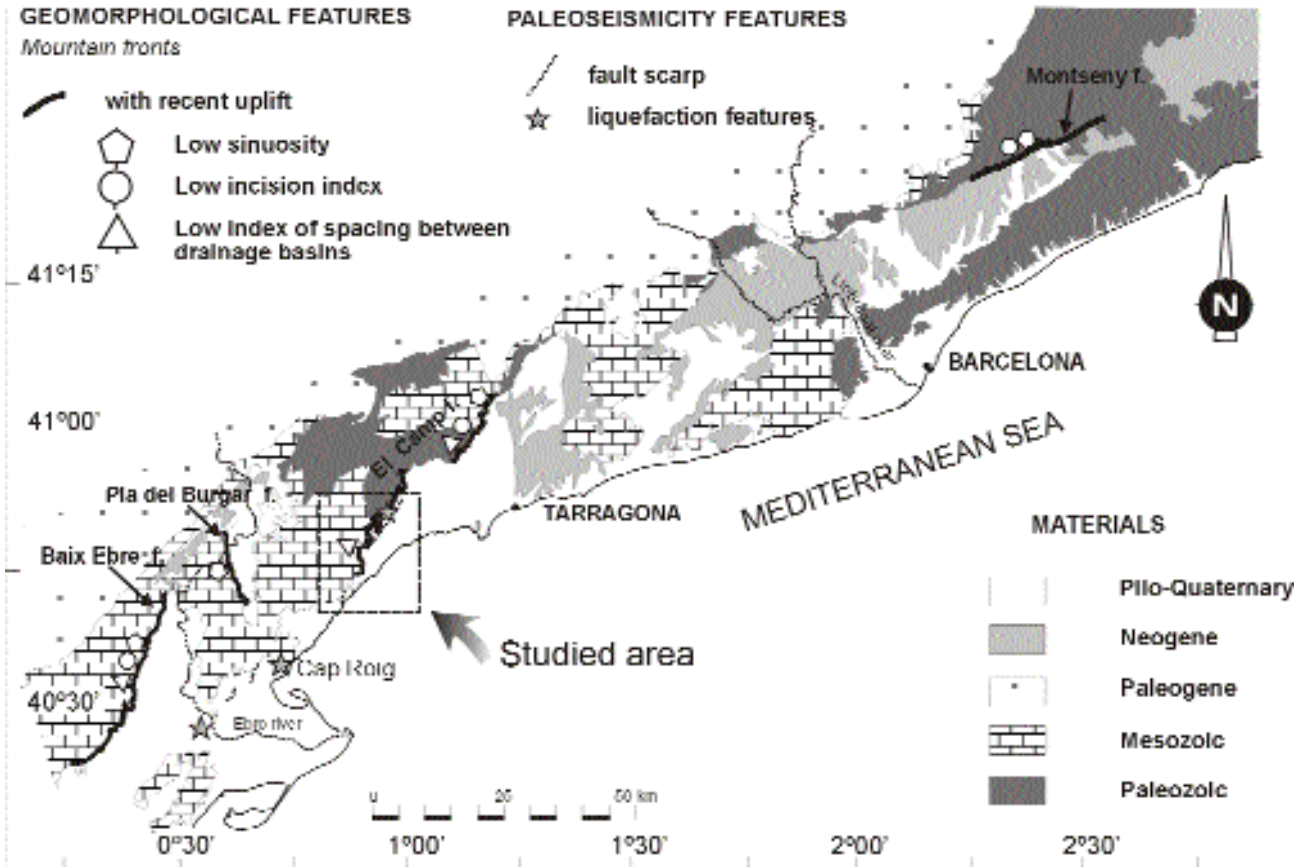

Figure 2. Geologic map of the Catalan Coastal Ranges with location of the active mountain fronts and some of their morphological activity indexes. Studied area contains part of the El Camp fault.

Figura 2. Mapa geológico de las Cadenas Costeras Catalanas con la situación de los frentes montañosos activos e indicación de los criterios geomorfológicos de actividad. El área estudiada contiene una parte de la falla de El Camp.

interpretations. This is why this fault was classified as an inactive fault and excluded from the seismic hazard analysis of the area.

Given their rare seismicity, the Catalan Coastal Ranges (Fig. 2), and, in particular, the El Camp fault zone, have been erroneously considered to be inactive. This is largely due to the absence of earthquakes with M>3.4 in this region in the period of instrumental recording. Moreover, none of the few earthquakes recorded in the vicinity since the XII century can be associated with the El Camp fault. The largest and nearest of these is the Tivissa earthquake (1845) with an epicentral intensity of VI-VII and with the epicenter located approx. 20 km west of the fault trace (Suriñach and Roca, 1982). This earthquake cannot be generated by the El Camp fault given that it dips towards the E. The surroundings of the El Camp fault can, thus, be regarded as a seismically silent area.

However, studies using geomorphologic, stratigraphic and tectonic approaches demonstrate that the area has experienced tectonic activity in recent times (Masana, 1995, 1996). These studies reveal four mountain fronts (Montseny, El Camp, Plà del Burgar and Baix Ebre) with evidence of recent uplift in the range (Fig. 2): 1) the lowest -with respect to the Catalan coastal ranges- values of sinuosity (S=1,2-1,5), 2) the highest values of valley entrenchment, 3) the highest convexity along profiles that are orthogonal to the front, 4) the most elongated and wine glass shaped basins (0,42-1,40), 5) well preserved multi-generation faceted spurs, and 6) the highest number of faults and flexures on recent sediments. Therefore, despite slow uplifting velocity, the faults have recently undergone activity. The analysis also reveals several scarps located at the foot of the El Camp and the Baix Ebre mountain fronts, cutting through Quaternary alluvial fans. The longest is at the

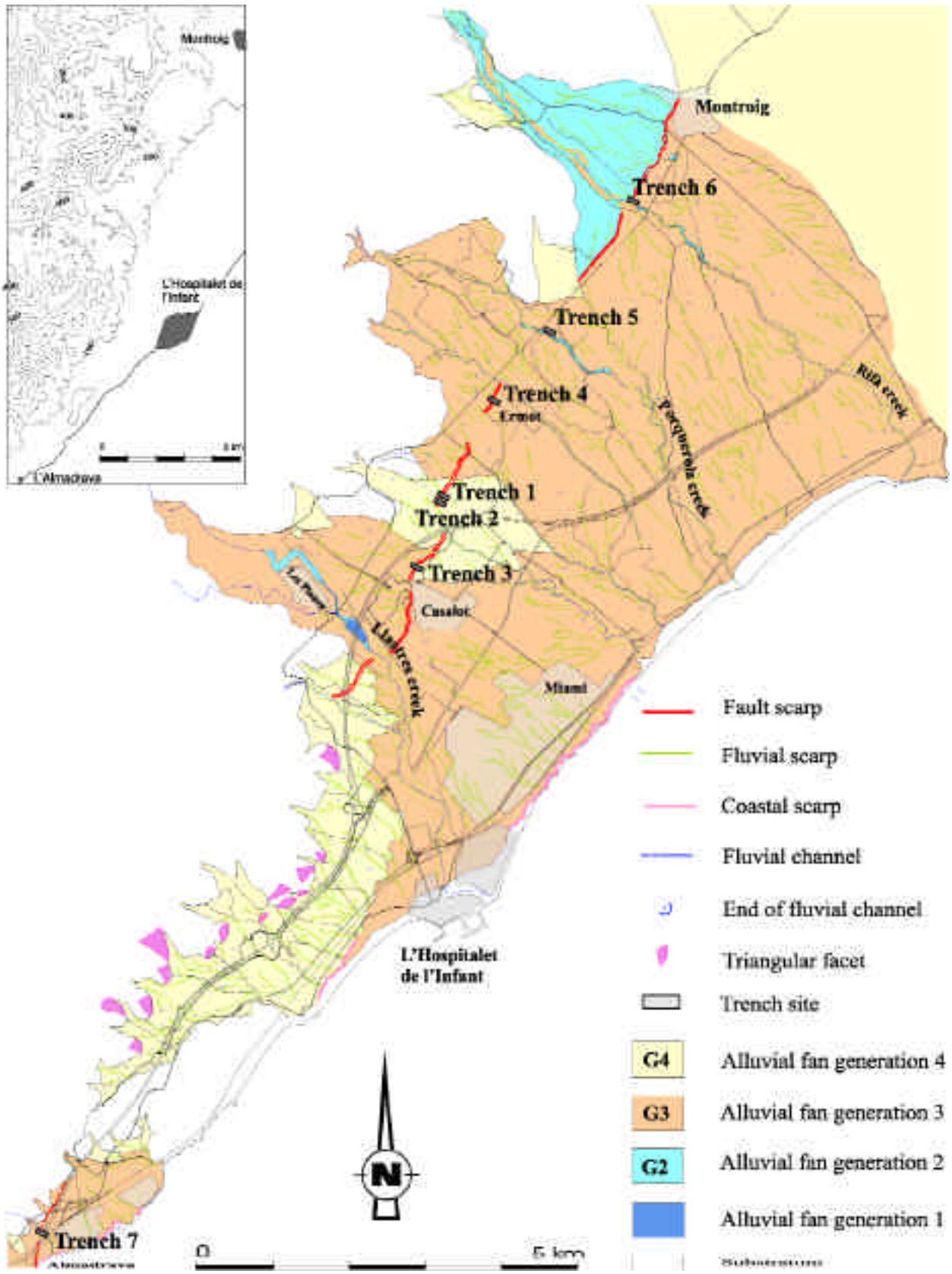
Montroig
L'Hospitalet de l'Infant
L'Ametlla
Montroig
Trench 6
Trench 5
Trench 4
Ermot
Trench 1
Trench 2
Trench 3
Casalot
Miami
Pesquerola creek
Riera creek
La Parra
Llauders creek
L'Hospitalet de l'Infant
Trench 7
Fault scarp
Fluvial scarp
Coastal scarp
Fluvial channel
End of fluvial channel
Triangular facet
Trench site
G4
Alluvial fan generation 4
G3
Alluvial fan generation 3
G2
Alluvial fan generation 2
Alluvial fan generation 1
N
0
5 km

foot of the El Camp mountain front and has been interpreted as a fault scarp for the following reasons: its location, its length (25 km onshore), its linearity and its varied topographic elevation. This refutes other interpretations such as a gravitational movement or an old shore line (Masana, 1995, 1996). Furthermore, the fault was observed in some creeks across the scarp. This author also concludes that the El Camp fault, which produced the scarp (attaining 17 m in Quaternary sediments), is an active fault since it cuts an alluvial fan generation yielding a Musterian lithic industry (not older than 100 ka). Thus, despite the absence of historical seismicity, there is solid evidence of current tectonic activity along the El Camp fault.

A paleoseismological analysis along the El Camp fault was undertaken to characterize its seismic behavior, i.e. to ascertain whether it was a seismogenic fault or not and to determine its seismic parameters (i.e. geometry of the fault and possible segmentation, maximum expected earthquake, elapsed time, slip rate and inter-seismic period) which would better constrain the seismic hazard of the area near the fault. The geomorphological approach was, therefore, employed to focus attention on small areas where paleoseismology could be applied; in this case along the El Camp fault.

GEOLOGICAL SETTING

The El Camp fault, which is composed of two en echelon faults (the northern and the southern El Camp faults), is part of a system of NE-SW crustal faults that form the Catalan Coastal Ranges (Fig. 2). The Neogene tectonic activity along the Catalan Coastal Ranges is the result of an E-W extension, perpendicular to the El Camp fault, which dates from the Oligocene-Miocene (Fontboté et al., 1990, Mauffret et al., 1973, Roca and Guimerà, 1992, Banda and Santanach, 1992). This extension is linked to the rift system of western Europe. The normal movement along the faults in the Catalan Coastal Ranges has led to the formation of a number of half-graben basins infilled with Neogene sediments.

The El Camp basin is bounded by the El Camp fault on the Northwest. The Neogene infilling of the basin is continental at the base, changing gradually to marine and subsequently to continental at the top. The Quaternary deposits are formed mainly by alluvial fans. The thickness of the infilling attains 1400 m near Reus (Lanaja 1987, Anadón et al., 1983). The studied fault

Figure 4. Liquefaction feature at Porquerola creek, several meters to the Northwest of the fault. Fine-sandy matrix-supported gravels overlain by conglomerates intrude into the latter forming a clastic dike. Younger gravels seal the structure on top.

Figura 4. Estructura de licuefacción en el barranco de Porquerola, algunos metros al noroeste de la falla. Gravas soportadas por arenas finas intruyen en los conglomerados suprayacentes y forman un dique clástico. Gravas más recientes sellan la estructura por su parte superior.

Figure 3. Geomorphologic map of the area cut by the El Camp fault scarp, south of Montroig, where the paleoseismological analysis was focussed. To the North of this town the footwall of the scarp is on granite.

Figura 3. Mapa geomorfológico del área cortada por el escarpe de falla de El Camp, al sur de Montroig, donde se centró el análisis paleosismológico. Hacia el norte de esta localidad, en el bloque inferior de la falla, aflora granito.

Figure 5. The El Camp fault scarp at trenches 1 and 2 on the G4 generation alluvial fans. For scale a person is standing on the lower and another on the upper inflexion point of the scarp to show 3.5 m of vertical displacement at this point.

Figura 5. El escarpe de falla de El Camp en la localidad de las trincheras 1 y 2 sobre un abanico aluvial de la generación G4. Se ha situado una persona en el punto de inflexión superior del escarpe y otra en el inferior para mostrar los 3,5 m de desplazamiento vertical en este punto.

scarp is situated along the southern fault of the en echelon fault system that constitutes the El Camp fault. Henceforth we shall refer to the southern El Camp fault as the El Camp fault.

APPROACH

A detailed geological study of the surficial units was performed as a preliminary step. This included a geomorphological and geological study with aerial photographs at different scales (1:18,000, 1:33,000, 1:70,000), topographic maps at different scales (1:5000, 1:25,000, 1:50,000) and field investigations. A stratigraphical analysis of the main geological units was also performed to detect different units and to date them.

Dating of the alluvial fans

An attempt was made to date both the surficial units and the buried units exhumed in the trenches. A correlation of the alluvial fan filling sequences with the most recent oxygen isotopic stages indicating sea-level high-stands was carried out. We also correlated them with the paleo-magnetic stages and observed that the target sedimentary units were younger than the Matuyama-

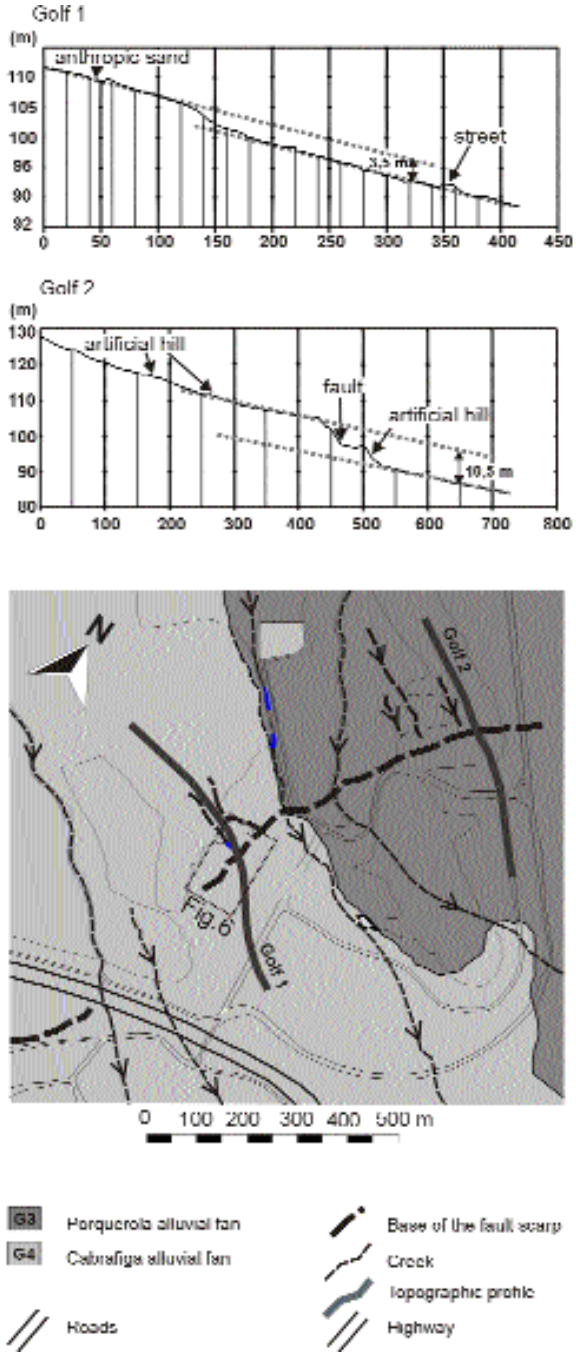

Figure 6. Geologic map of the golf course where the site for trenches 1 and 2 was selected. Topographic profiles across the fault scarp indicate a higher vertical offset across the older alluvial fan (10.5 m) than across the younger one (3.5 m).

Figura 6. Mapa geológico del campo de golf donde se seleccionó la localidad para excavar las trincheras 1 y 2. Los perfiles topográficos a través del escarpe de falla indican una mayor dislocación a través del abanico más antiguo (10,5 m) que a través del más reciente (3,5 m).

Brunhes boundary (780,000 yr). Accordingly, some radiometric methods (U/Th and thermoluminiscence) were selected for use mainly on carbonated layers (calcrete soils on top of the alluvial fans). Up to 50 samples were collected and dated with each of the two methods. The results were analyzed considering all possible errors such as sampling, methodological or context errors, and approximately half of the results were rejected (see Villamarín et al., 1999 for further methodological procedures). This provided us with an absolute age for the oldest calcrete soils on top of the alluvial fans, thereby yielding an insight into the age of the fans.

Site selection and tr enching

Sites for trenching were chosen preferentially on the youngest sediments. Some sites were also selected on the remaining Quaternary sediments in order to constrain the time interval represented by the deposits cut by the fault on the surface. In greater detail, geomorphological analysis was performed with the help of micro-topographic maps and profiles leveled with a total station (Leica 1700). This analysis yielded information on the most recent processes of deposition and erosion and was, thus, crucial in the site selection process. The best sites were those with an equilibrium between the rates of deformation, erosion and deposition: high erosion rates would have removed evidence of paleoearthquakes, and high depositional rates would have buried evidence of paleoearthquakes too deep to be analyzed with conventional trenching.

Trenches were dug with an excavator equipped with a hydraulic hammer because of the high cementation of the deposits on account of the carbonates and calcretes. Owing to their hardness, the width of the trenches exceeded 3 m so as to allow the excavator to operate. Trench walls were logged carefully at a scale of 1:20 and all calcrete soils were sampled for U/Th and TL dating. Some fine detritic layers were dated by TL; all soft layers were sampled for pollen analysis, and some fine soils, shells and charcoal pieces were employed for radiocarbon dating.

REGIONAL GEOMORPHOLOGICAL ANALYSIS

The regional geomorphological analysis performed on the upper sedimentary units filling up the El Camp basin in this area shows up to four generations of alluvial fans in the surroundings of the faulted area (Fig. 3). The criteria used to differentiate the alluvial fan generation were as follows: the level of surficial degradation, the level of cementation and the large unconformities observed between them. The oldest (G1) generation does not crop out in contact with the fault and does not contribute to the reconstruction of the recent deformation history of the fault; it will,

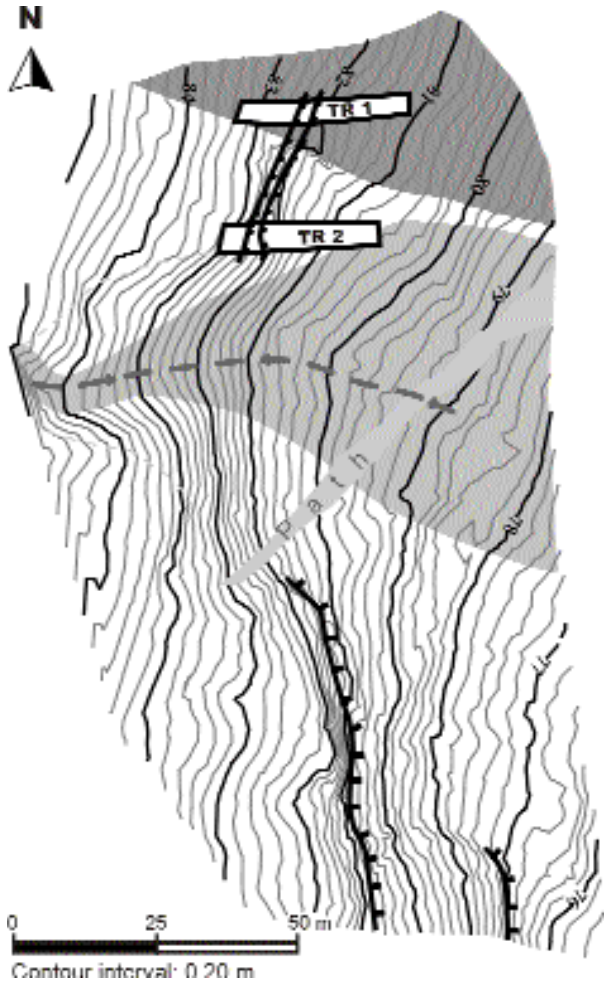

Figure 7. Micro-topographic map of the site area of trenches 1 and 2 with location of the fault scarp base knick, the trenches and the faults observed in the trenches. Dark gray in the NE represents a young sedimentary unit that apparently seals the fault. Lighter gray indicates the current sedimentation area in front of the small gully that erodes the fault scarp.

Figura 7. Mapa microtopográfico del área de las trincheras 1 y 2 con la situación de la línea de knick de la base del escarpe, las trincheras y las fallas observadas en las trincheras. El gris oscuro en el NE del mapa representa una unidad sedimentaria reciente que aparentemente sella la falla. El color gris más claro indica el área de sedimentación actual frente a una pequeña vaguada que erosiona el escarpe de falla.

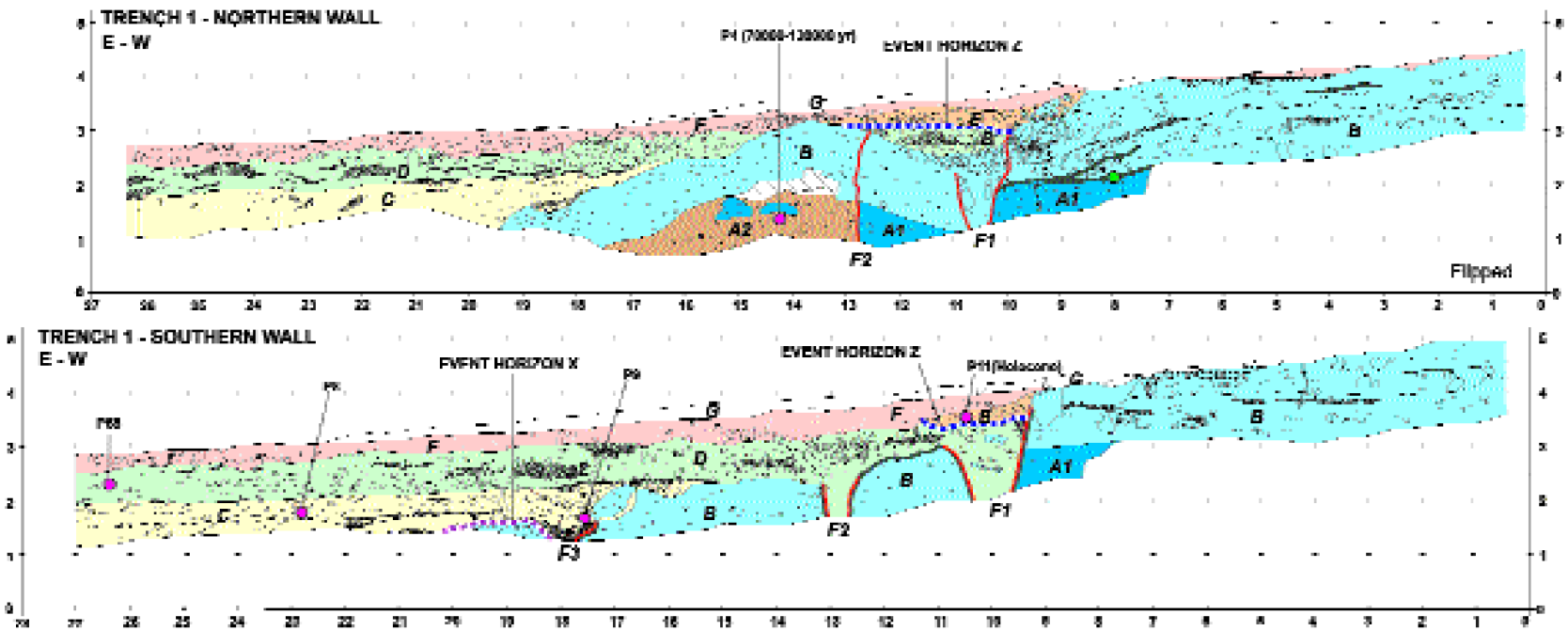

Ç Sand, anthropically deposited in relation to the golf course.

F Silt and clay, dark brown in color, corresponding to the subcurrent soil.

C Unconsolidated matrix supported gravel with some decimetric sharp clasts near the fault zone. Colluvial wedge.

D Unconsolidated matrix-supported gravel of fluvial origin.

c Unconsolidated matrix-supported gravel with sand levels. Fluvial origin.

B Strongly cemented and poorly selected matrix supported carbonatic conglomerates. Decalcification processes in the upper part of the unit. Extensive laminar caliche at top.

A Strongly cemented and poorly selected matrix supported conglomerates.

Decalcified limestones

Figure 8. Log of trench 1. Colored circles represent samples for dating (red: U/Th, green: TL, yellow: radiocarbon, pink: pollen). Thick red lines denote faults. Thick green lines indicate calcrete soils. Legend:
A1: Strongly cemented matrix-supported conglomerates. Clasts are carbonated, subangular, moderately sorted, and range from a few centimeters to a few decimeters in size. The matrix ranges from silt to sand and is pinkish in color. Cement is carbonated. Locally decalcified in the upper part of the unit. Laminar caliche on top.
A2: Poorly sorted, unconsolidated sand and silt, dark brown in color. The unit contains a small number of clasts. Clasts are carbonated in composition, subangular to subrounded, and range from a few centimeters to a few decimeters in size. Some are composed of subangular pieces of breccia proceeding from unit A1.
B: Strongly cemented and poorly sorted matrix-supported conglomerates. Clasts are carbonated, poorly classified, and range from a few centimeters to a few decimeters in size. The matrix ranges from silt to sand and is yellowish in color. Decalcification processes occurred in the upper part of the unit. Extensive laminar caliche on top, and oolitic caliches inside the unit.
C: Unconsolidated matrix-supported gravel. Clasts are carbonated in composition, subrounded, moderately sorted, and range from a few millimeters to a few decimeters in size. The matrix ranges from silt to sand. The gravel shows a fluvial architecture.
D: Unconsolidated matrix-supported gravel. Clasts predominate in the lower part of the unit, are carbonated, subangular, and range from a few millimeters to a few decimeters in size. The matrix ranges from silt to sand and is light brown in color.
E: Unconsolidated matrix-supported gravel. Clasts are carbonated, subangular, and mainly centimeter-size, although some decimeter-size clasts are found close to the fault. Matrix ranges from silt to sand and is reddish brown in color. Presence of modern roots.
F: Silt and clay, dark brown in color, corresponding to the present soil. Scarce carbonated, subrounded clasts ranging from a few millimeters to a few decimeters in size. $CaCO_3$ nodules.
G: Sand deposited by man for the golf course.
R1: Karstic-porosity fill. Reddish brown clay. This unit contains pieces of charcoal and few clasts ranging from a few centimeters to a few decimeters in size.
R2: Karstic-porosity fill. Dark brown clay. This unit contains carbonated, centimeter-size clasts, some of which (pieces of unit A) reach a few decimeters in size. Gastropod shells were found at the top of the unit.
R3: Karstic-porosity fill. Dark brown clay with granular fabric. This unit contains some carbonated, subrounded, centimeter-size clasts and yields pieces of charcoal and gastropod shells.

Figura 8. Secciones de la trinchera 1. Los círculos coloreados representan muestras para dataciones (rojo: U/Th, verde: TL, amarillo: radiocarbono, morado: polen). Las líneas rojas gruesas indican las fallas. Las líneas verdes gruesas indican calcretas. Leyenda:
A1: Conglomerados soportados por la matriz fuertemente cementados. Los clastos son carbonáticos, subangulosos, moderadamente seleccionados y sus dimensiones de centimétricas a decimétricas. La matriz va de limosa a arenosa y es de color rosado. El cemento es carbonático. Esta unidad está parcialmente decalcificada en su parte superior. Caliche laminar a techo.
A2: Arenas y limos no consolidados, pobremente seleccionados, de color marrón oscuro. Esta unidad contiene unos pocos clastos. Éstos son carbonáticos, de subangulosos a subredondeados, y sus dimensiones de centimétricas a decimétricas. Algunos están compuestos por fragmentos subangulosos de brecha procedente de la unidad A1.
B: Conglomerados soportados por la matriz, pobremente seleccionados y fuertemente cementados. Los clastos son carbonáticos, pobremente clasificados y sus dimensiones de centimétricas a decimétricas. La matriz, de limosa a arenosa, es de color amarillento. Presenta decalcificaciones en la parte superior de la unidad. Caliche laminar ampliamente desarrollado a techo y caliches oolíticos en el interior de la unidad.
C: Gravas no consolidadas, soportadas por la matriz. Los clastos son carbonáticos, subredondeados, moderadamente seleccionados, y sus dimensiones de milimétricas a decimétricas. La matriz es limosa a arenosa. Las gravas presentan una arquitectura fluvial.
D: Gravas no consolidadas, soportadas por la matriz. Los clastos predominan en la parte inferior de la unidad, son carbonáticos, subangulosos y sus dimensiones de milimétricas a decimétricas. La matriz, limosa a arenosa, es de un color marrón claro.
E: Gravas no consolidadas, soportadas por la matriz. Los clastos son carbonáticos, subangulosos, mayoritariamente de tamaño centimétrico, aunque se encuentran clastos de varios decímetros cerca de la falla. La matriz, limosa a arenosa, es de color marrón rojizo. Presencia de raices actuales.
F: Limos y arcillas de color marrón oscuro que corresponden al suelo actual. Escasos clastos carbonáticos, subredondeados, de dimensiones milimétricas a decimétricas. Nódulos de $CaCO_3$.
G: Arenas depositadas para la construcción del campo de golf.
R1: Relleno de la porosidad cárstica. Arcillas marrón rojizas. Esta unidad contiene fragmentos de carbón y unos pocos clastos de dimensiones milimétricas a decimétricas.
R2: Relleno de la porosidad cárstica. Arcillas marrón oscuro. Esta unidad contiene clastos carbonáticos, centimétricos, algunos de los cuales (fragmentos de la unidad A) alcanzan unos pocos decímetros. Se han encontrado conchas de gasterópodos en la parte superior de esta unidad.
R3: Relleno de la porosidad cárstica. Arcillas marrón oscuro con fábrica granular. Esta unidad contiene algunos clastos carbonáticos, centimétricos, subredondeados y ha suministrado fragmentos de carbón y conchas de gasterópodos.

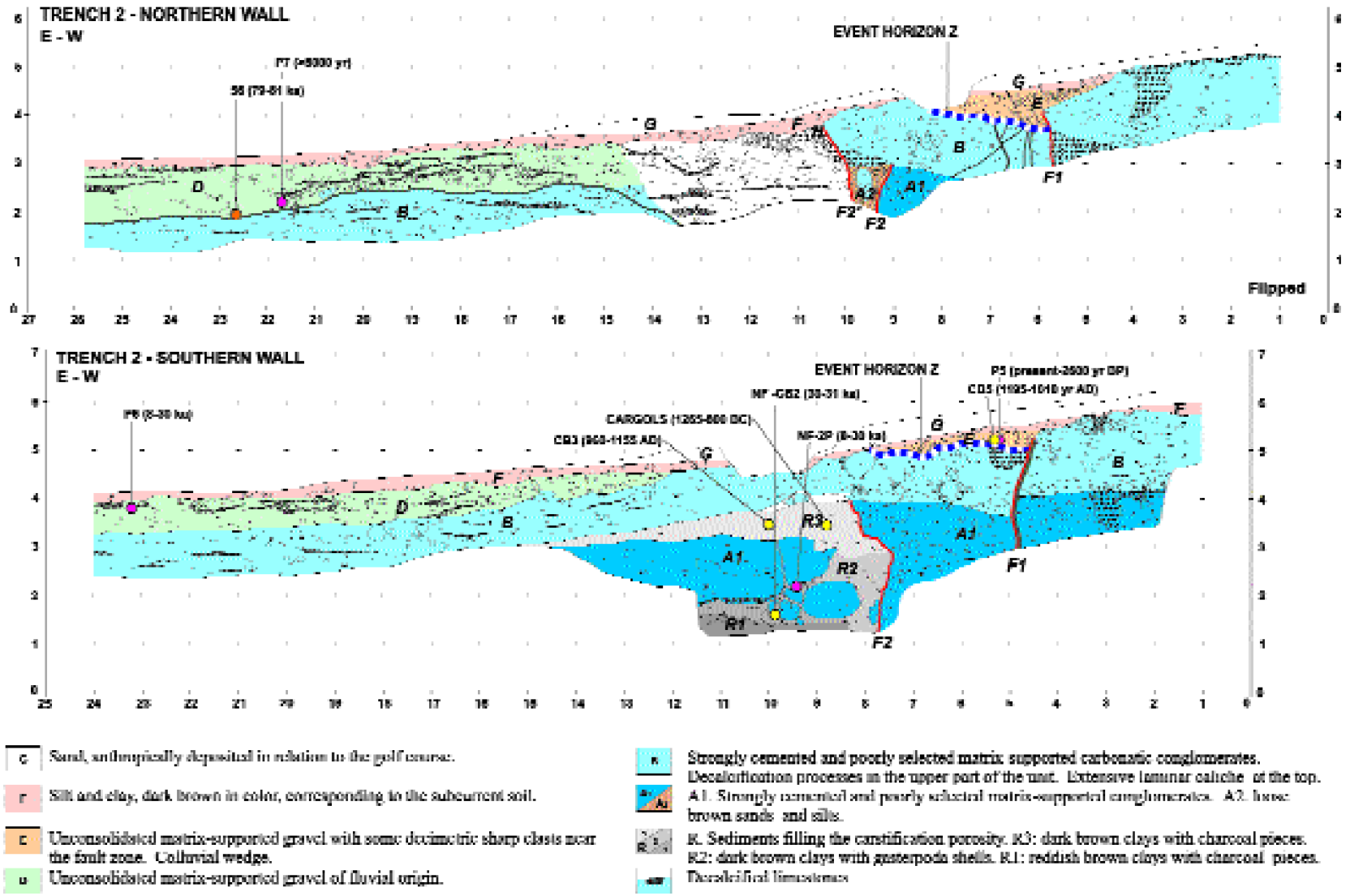

Figure 9. Log of trench 2. Colored circles denote samples for dating (red: U/Th, green: TL, pink: pollen, yellow: radiocarbon). Thick red lines indicate faults. Thick green lines represent calcrete soils. Same legend as for trench 1 (Fig. 8).

Figura 9. Secciones de la trinchera 2. Los círculos coloreados indican muestras para dataciones (rojo: U/Th, verde: TL, morado: polen, amarillo: radiocarbono). Las líneas rojas gruesas indican las fallas. Las líneas verdes gruesas indican calcretas. Misma leyenda que para la trinchera 1 (Fig. 8).

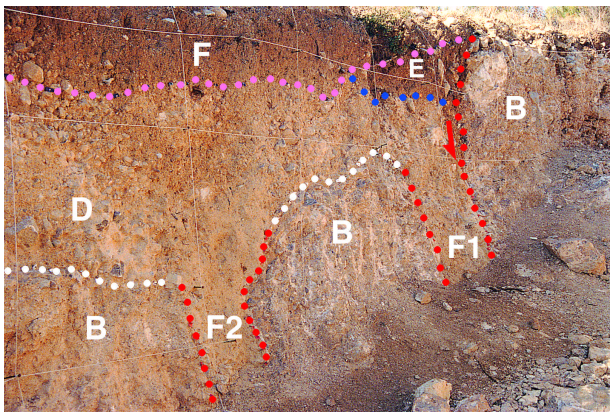

Figure 10. Overview of the southern wall of trench 1. Top of unit B is indicated by white flags and is dislocated by fault F1 in the background. Fault F2, in the foreground, is represented by a filled crack.

Figura 10. Vista general de la pared sur de la trinchera 1. El techo de la unidad B, señalado con banderitas blancas, está dislocado por la falla F1, en último término. La falla F2, en primer término, está representada por una grieta rellena con sedimentos.

therefore, not be considered in this paper. The alluvial fans of the G2 and G3 generations (Fig. 3) probably reached sea level at the time of the sedimentation of their top layers. This enables us, as a hypothesis, to correlate the age of the top layers of G2 with oxygen isotope stage 9 -which is around 300 ka BP- and also to correlate the age of the top layers of G3 with substage 5E -which is 125 ka BP-. G4 did not have the sea as a base level (it is currently at some distance from the sea shore) and, consequently, the same reasoning could not be applied to it. G4 is certainly younger than G3 given that it is deposited over it. Further radiometric dating (U/Th and TL) of the calcrete soils on top of G2 and G3 revealed that these are not younger than 300 ka and 125 ka, respectively, which is in agreement with the oxygen isotope correlation hypothesis (Villamarín et al., 1999).

The fault scarp is not continuous. It appears in the morphology several kilometers north of Montroig (Fig. 3), where the up-thrown block of the fault is made up of Variscan granites while the down-thrown block is composed of Quaternary alluvial fans. The scarp cuts through these Quaternary fans from Montroig to the proximity of Llastres creek and, further south, it transects the Mesozoic limestone bedrock for several kilometers (Fig. 3). To the South, in the Almadrava area, the scarp reappears for less than a kilometer

Table 1. Ages attributed to the trench samples after analyzing them with different dating techniques: pollen analysis, thermoluminescence, uranium series and radiocarbon. Location of the samples is shown on the logs by the sample code.

Tabla 1. Edades atribuidas a muestras de las trincheras después de analizarlas con diferentes técnicas: análisis polínico, termoluminiscencia, series del uranio y radiocarbono. La situación de las muestras se indica en las secciones de las trincheras con círculos de distintos colores según la técnica.

Pollen			
sample code	**age (BP)**	**location**	
P11	Holocene	TR1S	
P4	70-130ka	TR1N	
P6	8-30ka	TR2S	
P5	0-2600yr	TR2S	
NF2P	8-30ka	TR2S	
P7	older than 8 ka	TR2N	
P13	70-130ka	TR3S	
P48	70-130ka	TR3S	
P15	8-30ka	TR3S	
P28	Holocene	TR4N	
P29	Holocene	TR4N	
Thermoluminescence			
sample code	**age (yr BP)**	**location**	**material**
31	14,5032+/-10,360	TR7S	laminar caliche
33	66,647+/-8740	TR7S	laminar caliche
34	93,165+/-8949	TR7S	laminar caliche
27	258,348+/-22,210	TR7S	laminar caliche
U/Th			
sample code	**age (yr BP)**	**location**	**material**
56	80,671+/-1200	TR2N	laminar caliche
75	138,035+/-6000	TR3S	laminar caliche
Radiocarbon			
sample code	**age (yr BP)**	**location**	**material**
	conventional ^{14}C age		
NF-CB2	31,030+/-460 BP $^{13}C/^{12}C$= -26,3	TR2S	charcoal
2 sigma calibrated age (95% probability)			
CB3	960-1155 AD	TR2S	charcoal
CG4	250-530 AD	TR3S	gastropod shell
CB5	1195-1010 AD	TR2S	charcoal
TR2CARGOLS	1265-800 BC	TR2S	gastropod shell
CB3	1460-1670 AD	TR3S	charcoal

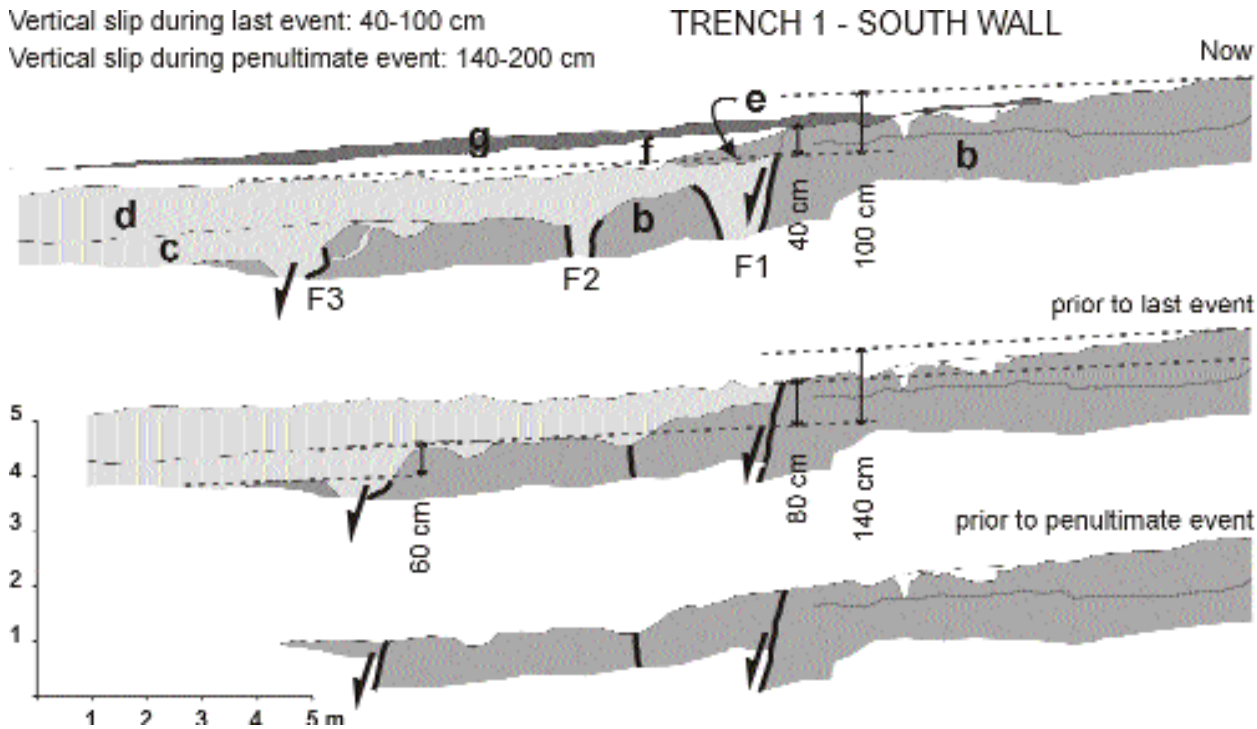

Figure 11. Restoration of the deformation produced by the two seismic events identified on the southern wall of trench 1, with the range of vertical displacement obtained for each event.

Figura 11. Restitución de la deformación producida por los dos eventos sísmicos identificados en la pared sur de la trinchera 1, con indicación de la ventana del desplazamiento vertical para cada uno de los eventos.

before entering the sea. This study concentrates on the portions of the scarp crossing recent sediments, i.e. southwest of Montroig. The scarp shows different relationships with the sedimentary units in the proximity of Montroig, where the G3 fans seal the fault and further south, near the sea, where even G4, the youngest fans, are deformed by the fault (see Fig. 3). These different relationships suggest a segmentation of the El Camp fault.

Regional and detailed field work in the faulted area provides considerable evidence of strong seismic shaking. At Montroig, and at Porquerola creek, at a distance of less than 20 m from the fault, are a number of liquefaction structures, mainly sand dikes (Fig. 2), which are related to movements of the El Camp fault since they follow fractures parallel to its strike (Fig. 4). Some liquefaction structures also crop out several kilometers away from the fault in Cap Roig (Fig. 2), where fine sands, which are susceptible to liquefaction caused by strong shaking, crop out. These structures suggest that the El Camp fault is seismogenic.

TRENCHING

Seven trenches were analyzed (location in Fig. 3). All of them, except for trench 6, were excavated across a precisely located fault scarp. Trenches 1 and 2 were selected at the only preserved site where the youngest alluvial fan (G4) is cut by the fault. Trench 3 was dug where the fault separates the deposits of G3 from those of G4. Micro-geomorphological analysis was very useful in selecting the site for trench 4, which was dug on a G3 alluvial fan, where a very recent gully crosses the scarp. Trenches 5 and 6 were not planned for detecting paleoearthquakes but for better constraining the limits of the segment. Finally, trench 7 was an open outcrop where no site selection procedure was followed.

Trenches 1 and 2

Only part of the fault scarp cutting the last generation of alluvial fans (G4) is preserved from human modification. This part, which encroaches on a golf

course (Bonmont Terres Noves), provides evidence of the most recent deformation of the fault.

Site selection

Site selection followed a two-step process. Detailed mapping of the limits between the G3 and G4 alluvial fans was performed and the vertical displacement of each of these units was determined by microtopographic profiling across the fault scarp (Figs. 5 and 6). Although the fault scarp is still unmodified where it cuts the G4 alluvial fan at this site, human modification reaches some areas near the scarp. The part of the scarp crossing G3 in this area is very modified. For this reason, topographic profiles were measured over a long distance to avoid human activity and to obtain the original shape of the alluvial fan surface which is better preserved at some distance from the scarp (Fig. 6). The results are coherent because they show a vertical offset which is larger on the older fan (10.5 m) than on the younger fan (3.5 m). Next, the precise location of trenches 1 and 2 was selected. To this end, a detailed mapping of the superficial units was performed on a microtopographic base map (Fig. 7). The map reveals the exact position of the scarp (divided into two strands in the South) and its recent erosion by a small gully which carries some sediments to the small basin at the foot of the scarp. Furthermore, the scarp disappears to the North under a very recent colluvial unit (dark gray in Fig. 7). Trench 1 was dug across the scarp in this young unit that could seal the fault. Trench 2 was dug near the creek where an equilibrium existed between erosion and deposition. Both trenches were 26 m long, no more than 3 m deep, and oriented in an E-W direction (Figs. 8 and 9).

Trench analysis

Since the sedimentary units and structures in both trenches are correlatable, owing to their proximity, they are described together. As many as three fractures (F1, F2 and F3) are visible in trenches 1 and 2 (Figs. 8, 9 and 10). F1 and F3, which show a displacement of unit B, are formed by a planar structure and display imbricated clasts along them. F2 is an open crack and shows no vertical displacement of unit B except in the northern wall of trench 2.

Units A1 and B are composed of highly cemented alluvial fan deposits whereas units C and D are loose gravels with evidence of fluvial transport, possibly along the small gully shown on the microtopographic map in Fig. 7. Unit F is the present soil whereas G is a man-made layer made for the golf course. All these units are extensive in the trench walls; in contrast, unit E is a wedge shaped unit which is located only downslope of fault F1 and is made up of loose matrix-supported gravels containing large angular pebbles of limestone derived from unit B. Unit A2 has similar lithological characteristics but its real shape is not constrained because trench 1 was too shallow. Units R1, R2 and R3 (in trench 2) also have a limited extension and correspond to a karstic infilling in unit A1. Absolute dating of gastropod shells and charcoal in these units (table 1) shows very young correlative ages (2σ 95% probability calibrated results for charcoal samples in R3 indicate an age of 960-1155 yr AD and for continental gastropods 1265-800 yr BC) whereas the upper layers are two orders of magnitude older (U/Th radiometric dating indicates an extensive caliche soil formation on top of unit B in 125 ka BP).

Evidence for three seismic events was found on these four trench walls, from young to old: events Z, X and W:

Event Z: Unit E was interpreted as a colluvial wedge deposited at the foot of a partly eroded fault scarp along fault F1, visible on all trench walls. Hence, the base of this unit represents the horizon of event Z.

Event X: This is evidenced only on the southern wall of trench 1 by a buried scarp along F3 and also by the vertical dislocation of the top of unit B along F1 in trench 1 after restoring the dislocation caused by event Z (Fig. 11). This event was not observed on the other walls possibly because of the limited depth of the trenches. Faults F1 and F3 were activated during this event. The base of unit C is, therefore, event horizon X, although, in this case, the elapsed time between the event and the deposition of C could be a relatively long period since unit C is not a colluvial wedge but a broad fluvial unit.

Event W: The evidence for the oldest event W is weak. Unit A2, on the northern wall of trench 1, has colluvial wedge characteristics. Moreover, fault F2 is sealed by unit B. This suggests that there was a faulting event older than event X.

In order to chronologically constrain the identified events, absolute dating was performed on all suitable samples in both trenches as indicated by the colored circles in the trench logs (Figs. 8 and 9). The base of unit

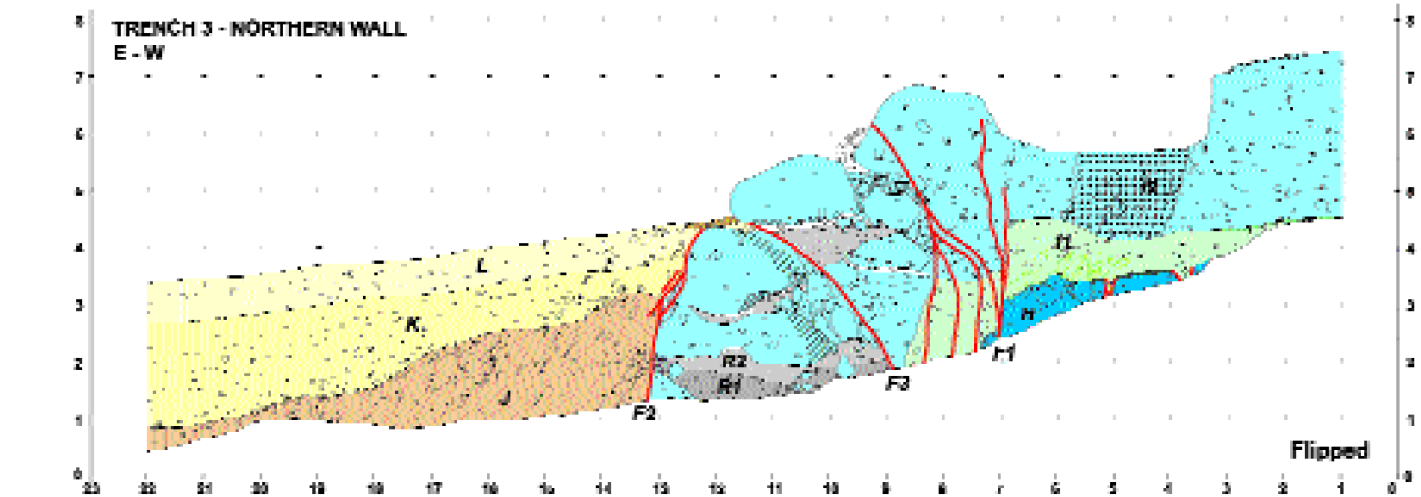

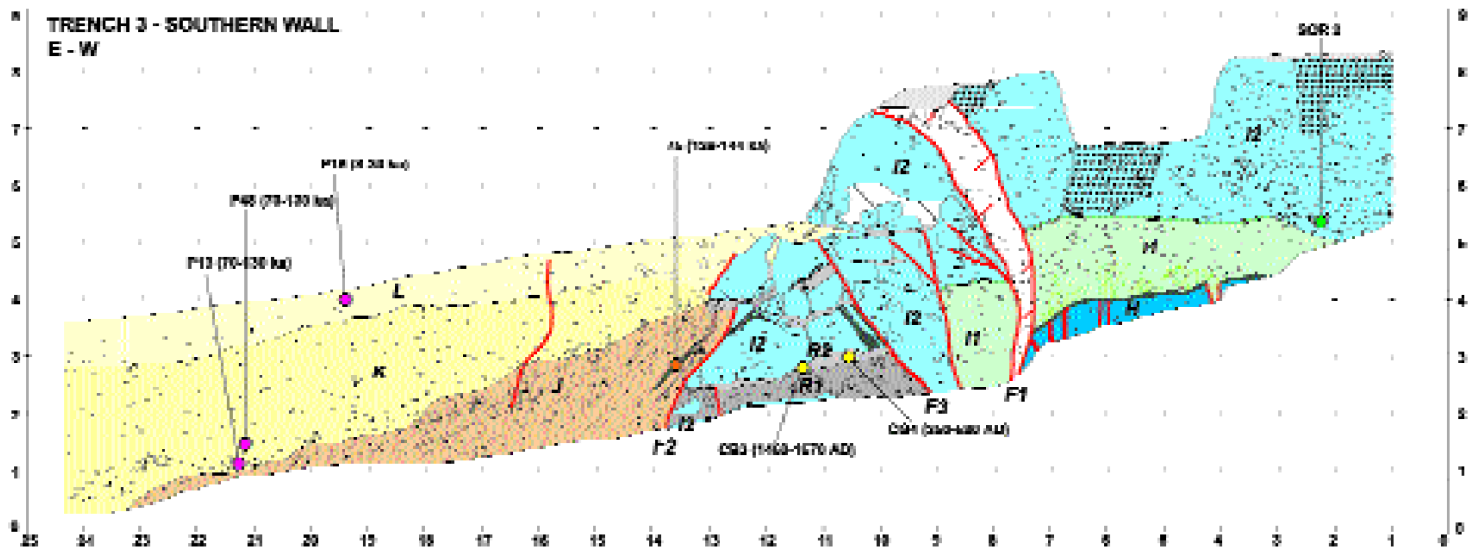

L — Unconsolidated clays and silts, dark brown in colour. Current soil at the top.

K — Little cemented matrix supported gravels with very few clasts.

J — Cemented matrix-supported conglomerates with internal caliches parallel to the oblique sets.

I — Moderately cemented clast-supported conglomerates, light brown in colour. Laminar caliche at top.

I — Unconsolidated pinky clays with an calcareous caliche at the bottom.

H — Strongly cemented, matrix-supported carbonate conglomerates.

R, R1, R2 — R: Sediments filling the carstification porosity. R2: Unconsolidated clays with a large amount of charcoal and gastropoda shells. R1:light brown unconsolidated clays with some pieces of charcoal the top.

Decalcified limestones

E, close in time to event Z, is between 1195 yr AD and 2600 yr BP according to samples CB5 and P5 of radiocarbon and pollen, respectively (table 1). The pollen content indicates an age older than 8000 yr for unit D (samples P6, P7), and the correspondence analysis between pollen samples of units D (P6, P7 and P68) and R1 (karstic infill, sample NF2P) shows a good correlation between these units. Hence, unit R1 may correlate in time with unit D. Since a radiocarbon dating on unit R1 (sample NF-CB2) gives an age of 31,030 +/- 460 yr BP, the best chronological bracket of event Z is then between 31,490 yr BP and 1195 yr AD although an age close to the latter is more likely (approx. 3000 yr BP).

The top of unit B is locally covered with a calcrete soil which yielded dates from 79,471 to 81,871 yr BP with U/Th (table 1). The soil post-dates the alluvial fan. Unit A2 is 70 to 130 ka old (in accordance with sample P4 pollen content) and, therefore, the top of unit B is constrained to the time interval between 130 ka and 79,417 yr BP. The regional analysis showed that

---

Figure 12. Log of trench 3. Colored circles indicate samples for dating (red: U/Th, green: TL, pink: pollen). Thick red lines denote faults. Thick green lines represent calcrete soils. Legend:
H: Strongly cemented matrix-supported conglomerates. Clasts are carbonated, subangular, do not show any sorting, and range from a few centimeters to a few decimeters in size. The matrix ranges from clay to sand and is pinkish in color. Laminar caliche on top. Vertical cracks are present.
I 1: Unconsolidated pinkish clays. Extensive caliche at the bottom showing a cracked fabric, caliche nodules in the central part of the unit, especially close to the fault, and a red clay level at the top.
I 2: Slightly cemented clast-supported conglomerates, light brown in color. Clasts are carbonated, subrounded, and range from a few centimeters to a few decimeters in size. Laminar caliche on top and inside the unit.
J: Cemented, matrix-supported conglomerates. Clasts are formed by limestone and conglomerates, are angular, decimeter-size, and moderately sorted. Internal architecture is defined by oblique sets. Caliche developed parallel to the sets.
K: Slightly cemented, matrix-supported conglomerates. Clasts are scarce, carbonated in composition, and range from a few centimeters to a few decimeters in size. The matrix ranges from clay to silt and is red in color.
L: Unconsolidated clays and silts, dark brown in color. Few carbonated, moderately sorted clasts ranging from subangular to subrounded. The current soil developed at the top of the unit contains a large number of live roots.
R 1: Karstic-porosity fill. Unconsolidated clays, light brown in color. They contain centimeter-size, subangular, poorly sorted, carbonated clasts, and pieces of charcoal at the top of the unit.
R 2: Karstic-porosity fill. Unconsolidated clays with only very scarce clasts. Clasts are carbonated, moderately sorted and range from a few millimeters to a few centimeters in size. They are more abundant in the upper part of the unit. This unit yields a large amount of charcoal, and gastropod shells. It contains live roots.

Figura 12. Secciones de la trinchera 3. Los círculos coloreados representan muestras para dataciones (rojo: U/Th, verde: TL, amarillo: radiocarbono, morado: polen). Las líneas rojas gruesas indican las fallas. Las líneas verdes gruesas indican calcretas. Leyenda:
H: Conglomerados soportados por la matriz, fuertemente cementados. Los clastos son carbonáticos, subangulosos, no están seleccionados y sus dimensiones son de centimétricas a decimétricas. La matriz, de arcillosa a arenosa, es rosada. Caliche laminar a techo. Se observan grietas verticales.
I1: Arcillas rosadas no consolidadas. Caliche ampliamente desarrollado en la parte inferior de la unidad con una fábrica agrietada, nódulos de caliche en la parte central, especialmente cerca de la falla, y un nivel de arcillas rojas a techo.
I2: Conglomerados soportados por los clastos ligeramente cementados, de color marrón claro. Los clastos son carbonáticos, subredondeados y sus dimensiones de centimétricas a decimétricas. Caliche laminar a techo y en el interior de la unidad.
J: Conglomerados soportados por la matriz, cementados. Los clastos están formados por calizas y conglomerados, son angulosos, decimétricos y moderadamente seleccionados. La arquitectura interna viene definida por sets oblícuos. Caliche desarrollado paralelamente a los sets.
K: Conglomerados soportados por la matriz, ligeramente cementados. Los clastos son escasos, de composición carbonática y sus dimensiones de centimétricas a decimétricas. La matriz, de arcillosa a limosa, es de color rojo.
L: Arcillas y limos no consolidados, de color marrón oscuro. Pocos clastos carbonáticos, moderadamente seleccionados, de subangulosos a subredondeados. El suelo actual desarrollado a techo de esta unidad contiene numerosas raices vivas.
R1: Relleno de la porosidad cárstica. Arcillas no consolidadas, de color marrón claro. Contiene clastos carbonáticos, pobremente seleccionados, subangulosos, de tamaño centimétrico y fragmentos de carbón en la parte alta de la unidad.
R2: Relleno de la porosidad cárstica. Arcillas no consolidadas con sólo muy escasos clastos. Los clastos són carbonáticos, moderadamente seleccionados y sus dimensiones de milimétricas a centimétricas. Son más abundantes en la parte superior de la unidad. Esta unidad ha suministrado gran cantidad de carbón y conchas de gasterópodos. Contiene raices vivas.

there was an important stage of calcrete soil development in the area 125 ka ago (Villamarín et al. 1999), which is consistent with the time range proposed for the calcrete soil in trenches 1 and 2. The age of this calcrete soil could be 125 ka and thus, event X would have occurred between 125 ka and 30,570 yr BP. Given that sample P6 is located at the top of unit D, a long period of time (deposition of units C and D) elapsed between the event and the age of P6; therefore, event X could considerably predate 30,570 yr BP. Event W is older than 125 ka, but is badly constrained in age since the age of the sediments prior to the event is unknown.

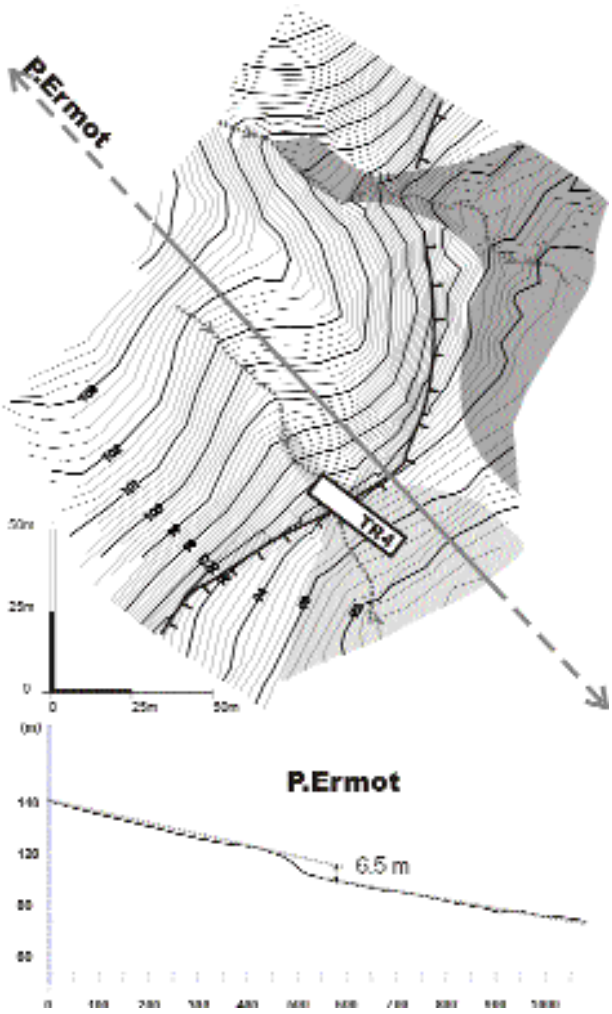

Figure 13. Micro-topographic map of the site of trench 4 and topographic profile leveled across the fault scarp at this site.

Figura 13. Mapa microtopográfico de la localidad de la trinchera 4 y perfil topográfico levantado a través del escarpe de falla.

Figure 14. Log of trench 4. Colored circles indicate samples for dating (red: U/Th, green: TL, pink: pollen). Thick red lines represent faults. Thick green lines denote calcrete soils. Legend: M: Highly cemented, matrix-supported conglomerates. Clasts are carbonated, slightly sorted, angular, and range from a few centimeters to a few decimeters in size. The matrix ranges from clay to silt and is pinkish in color. Laminar caliche on top. The north wall shows a clay bed interlayered with the conglomerates. This unit is made up of light brown clays containing subangular clasts of up to a few centimeters in size (green in the log). N: Unconsolidated, well sorted silts and clays light brown to orange in color, including some decimeter-size, carbonated clasts. O: Strongly cemented, poorly sorted, matrix-supported conglomerates. Clasts are carbonated, subangular to subrounded, and range from a few centimeters to a few decimeters in size. Locally weathered at the top and along the joints. Laminar caliche on top. P: Moderately consolidated, heterometric, matrix-supported conglomerates. Clasts are made up of pieces of conglomerates showing a facies corresponding to units O and M. They attain 40 cm in size, and they are strongly angular. The matrix ranges from clay to silt and is light brown in color. Q 1: Slightly consolidated, matrix-supported gravel. Clasts are carbonated, subangular, and moderately sorted. The matrix ranges from clay to silt and is light brown in color. Q 2: Unconsolidated, matrix-supported gravel. Clasts are very scarce. The matrix ranges from clay to silt. S: Unconsolidated clays, dark brown in color, containing some clasts ranging from 2 to 10 cm in size. The upper part of the unit corresponds to the present soil.

Figura 14. Secciones de la trinchera 4. Los círculos coloreados representan muestras para dataciones (rojo: U/Th, verde: TL, morado: polen). Las líneas rojas gruesas indican las fallas. Las líneas verdes gruesas indican calcretas. Leyenda: M: Conglomerados soportados por la matriz, altamente cementados. Los clastos son carbonáticos, ligeramente seleccionados, angulosos, y sus dimensiones de centimétricas a decimétricas. La matriz, de arcillosa a limosa, es de color rosado. Caliche laminar a techo. La pared norte muestra un lecho arcilloso intercalado en los conglomerados. Éste está constituido por arcillas de color marrón claro que contienen clastos subangulosos que alcanzan tamaños centimétricos (verde en la sección). N: Limos y arcillas bien seleccionadas, no consolidados, de color marrón claro a naranja y que incluyen algunos clastos carbonáticos de dimensiones decimétricas. O: Conglomerados soportados por la matriz, pobremente seleccionados, fuertemente cementados. Los clastos son carbonáticos, de subangulosos a subredondeados, y sus dimensiones de centimétricas a decimétricas. Localmente meteorizados a techo y a lo largo de las diaclasas. Caliche laminar a techo. P: Conglomerados soportados por la matriz, heterométricos, moderadamente consolidados. Los clastos están formados por fragmentos de conglomerados que muestran facies correspondientes a la unidades O y M. Alcanzan un tamaño de hasta 40 cm y son fuertemente angulosos. La matriz, de arcillosa alimosa, es de color marrón claro. Q1: Gravas soportadas por la matriz, ligeramente consolidadas. Los clastos son carbonáticos, subangulosos, y moderadamente seleccionados. La matriz, de arcillosa a limosa, es de color marrón claro. Q2: Gravas soportadas por la matriz, no consolidadas. Los clastos son muy escasos. La matriz es de arcillosa a limosa. S: Arcillas no consolidadas, de color marrón oscuro, con algunos clastos de 2 a 10 cm. La parte alta de la unidad corresponde al suelo actual.

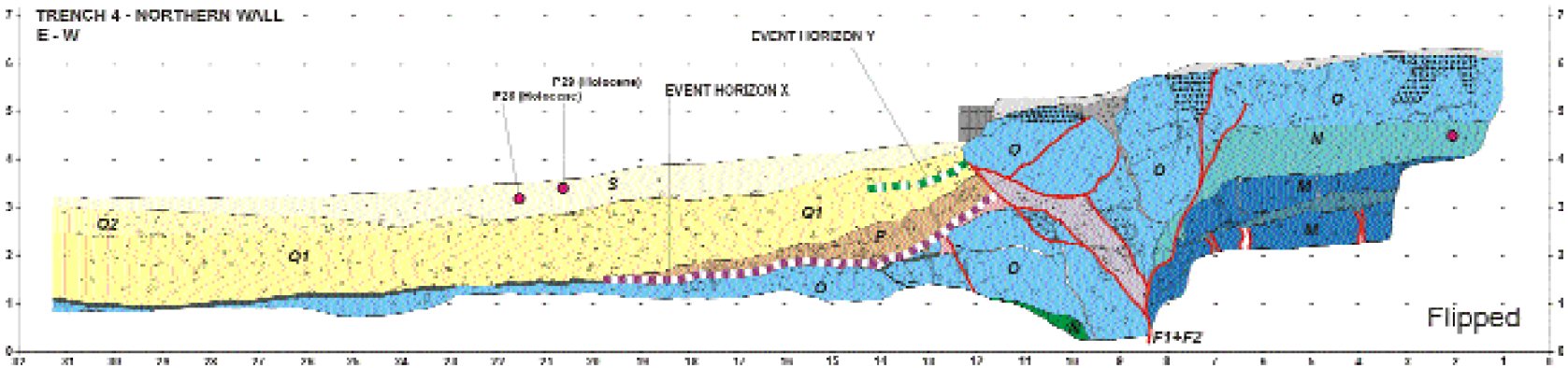

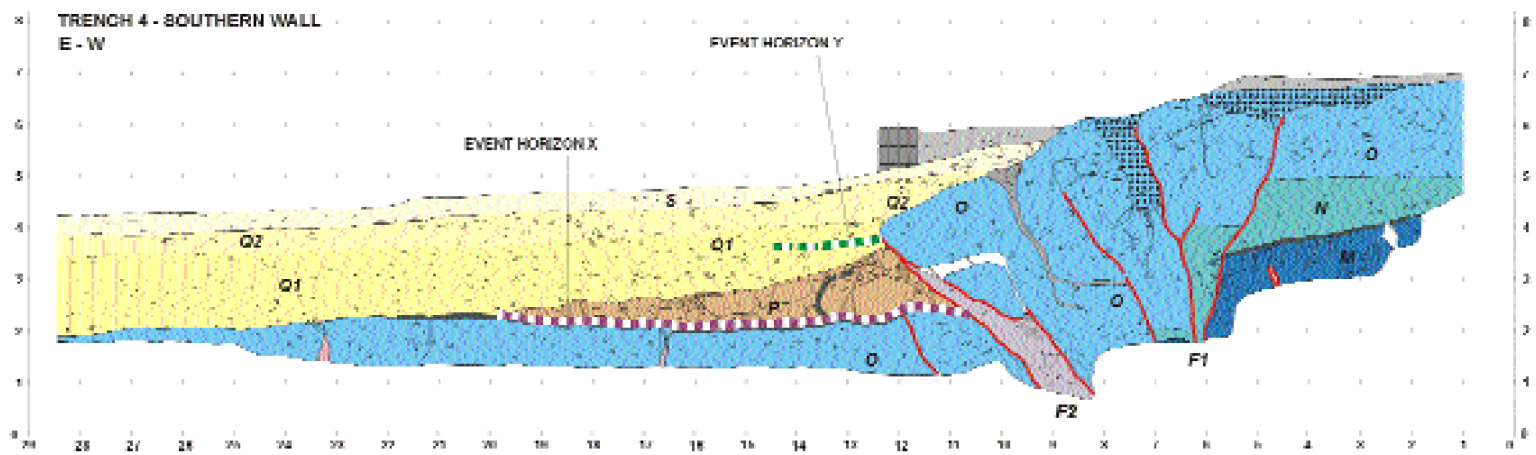

Unconsolidated clays, dark brown in color, containing some clasts ranging from 2 to 10 cm in size. The upper part of the unit corresponds to the current soil.

Unconsolidated, matrix-supported gravel. Clasts are very scarce. The matrix ranges from clays to silts.

Slightly consolidated, matrix supported gravel. Clasts are carbonatic, subangular, and moderately selected. The matrix ranges from clays to silts and is light brown in color.

Moderately consolidated, heterometric, matrix-supported conglomerates. Clasts are made of pieces of conglomerates showing facies corresponding to units O and M. Their size attains up to 40 cm, and is strongly angular. The matrix ranges from clays to silts and is light brown in color.

Strongly cemented, poorly selected, matrix-supported conglomerates. Clasts are carbonatic, subangular to subrounded, and range from a few centimeters to a few decimeters in size. Locally weathered at the top and along the joints. Laminar calliche at the top.

Unconsolidated, well selected silts and clays light brown, orange in color, including some decimeter-size, carbonatic clasts.

Highly cemented, matrix supported conglomerates. Clasts are carbonatic, poorly selected, angular, and range from a few centimeters to a few decimeters in size. Matrix ranges from clay to silty and is pinky in color. Laminar calliche at the top. The north wall shows a clay bed interlayered in the conglomerates. This unit is made up of light brown clays containing subangular clasts up to few centimeters in size.

Loose matrix supported gravels with silty and sandy matrix.

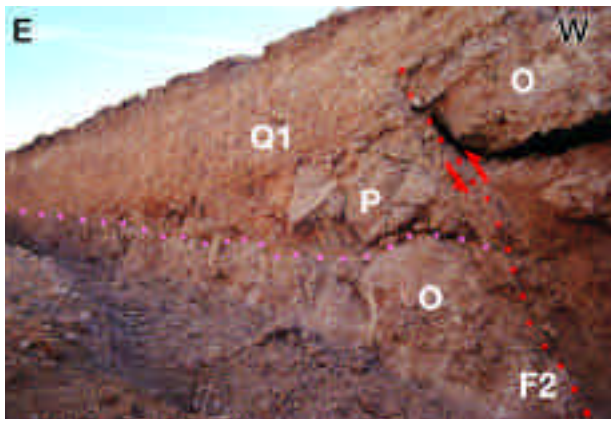

Figure 15. General view of the southern wall of trench 4 with fault F2 in the foreground over the colluvial wedge unit P. Unit P is composed of large blocks of cemented conglomerates and extends towards the background of the picture.

Figura 15. Vista general de la pared sur de la trinchera 4 con la falla F2 en primer término y por encima de la cuña coluvial P. La unidad P está compuesta por grandes bloques de conglomerados cementados y se extiende hacia el último término de la fotografía.

Trench 3

After excavating the only preserved part of the fault scarp on the G4 alluvial fans, we dug further south (Fig. 3) where the scarp crosses the G3 deposits but with the G4 sediments deposited in the down-thrown wall. This part of the scarp where the loose sediments of G4 were extracted is currently a quarry. Only a very narrow strip was still intact or with little human modification. Trench 3 was dug at this site in a WNW-ESE direction and with a length of 25 m and a depth of up to 5 m locally. Two long topographic profiles were leveled although their length was limited by the highway on the footwall. Considering these limitations, and reconstructing the modified landscape, the vertical topographic displacement of the fault scarp at this point was 8-9 m.

Trench 3 (Fig. 12) shows a 7 m wide deformed zone linked to the fault scarp. There are three faults in which the vertical displacement is concentrated. In the footwall, west of the faulted zone, sediments from alluvial fan G3 crop out with a highly cemented alluvial conglomerate (unit H) at the base, overlain by a fine-grained unit (I1), and a thick gravel unit (I2) on top. Although the gravel of unit I2 is loose in the trench outcrop, it shows a highly cemented layer at the top where the original surface of the fan has been preserved. In the hanging wall, the sedimentary units are matrix-supported gravels from alluvial fan generation G4 and are characterized by a low cohesion which decreases upwards. Unit J, at the base, displays eastward dipping sets of calcrete layers, suggesting a local extension of this unit. By contrast, units K and L have a wide lateral extension, indicating a broad deposition in the basin at the foot of the fault scarp. The deformed zone of the trench forms a breccia composed of large conglomerate blocks derived from unit I2, with high porosity, partially filled with loose silts and sands (Units R1 and R2). Radiometric dating of charcoal and gastropod shells in these loose sediments and palynofacies analysis indicate that they are extremely young (samples CB3 and CG4) compared with the host rocks. The observed karstic dissolution in some blocks and the infilling of high porosity observed on the southern wall of trench 2 suggest that the fault runs locally across a karstified area.

Although evidence of deformation is shown along all the mentioned faults in trench 3, evidence of discrete events of deformation is scarce. The shape and internal stratification of unit J may be attributed to a colluvial wedge deposited at the base of a previous scarp. The chronostratigraphical constraints on this event are limited. Sample 75 has an age of 138-144 ka, samples from unit K are 70-130 ka old and those from unit L are 8-30 ka old (Fig. 12 and table 1). Accordingly, the top of unit J (with calcrete in its upper part interpreted as having formed during the phase of calcrete formation, 125 ka ago) corresponds to the top of the G3 alluvial fans. Consequently, the seismic event that resulted in the deposition of the colluvial wedge J probably predates 125 ka.

Furthermore, reference levels inside the karstified unit I2 are dislocated by fault F3, which cuts unit L near the surface. Despite the scant evidence, this would indicate an event affecting unit L (possibly correlating with event Z in trenches 1 and 2), which occurred after 30 ka BP (sample P15).

Trench 4

Site selection

Once all the possible sites on the G4 alluvial fans were investigated, the sites situated on the G3 fans were explored for further trenching. Trenching in these older sediments may also yield information on very recent events if the site is correctly selected in areas of recent local deposition. To the South of trench 3, the scarp is

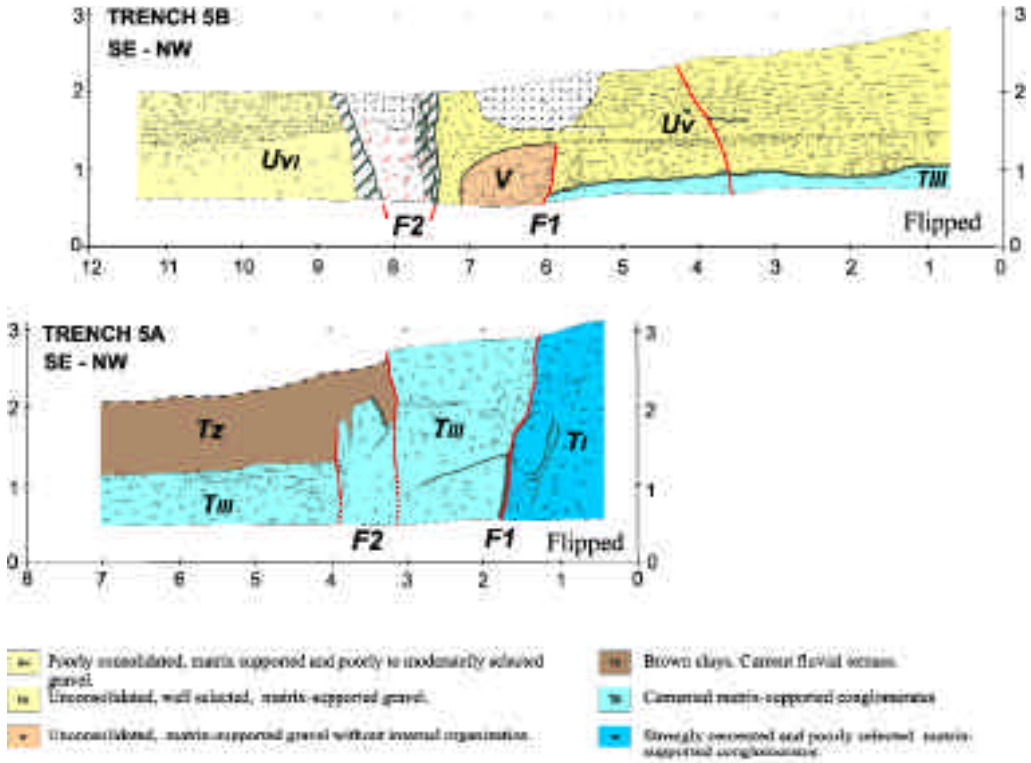

Figure 16. Log of trench 5 whose units form part of G3. Thick green lines indicate calcrete soils. Legend: T 1: Strongly cemented, matrix-supported conglomerates. Clasts are carbonated, poorly sorted, range from subrounded to rounded in shape and from a few centimeters to a few decimeters in size. The matrix ranges from clay to sand and is pinkish in color. There are plenty of laminar and oolitic caliche crusts inside the unit. Oolitic caliche on top. T III: Well cemented, matrix-supported conglomerates. Clasts are carbonated, centimeter-size, and show a moderate to good sorting. The matrix ranges from clay to sand and is light brown in color. U V: Unconsolidated, well sorted, matrix-supported gravel. Clasts are carbonated, subrounded, centimeter-size, occasionally decimeter-size. The number of clasts decreases towards the top. Preferred location of clasts defines internal lamination. The matrix ranges from clay to silt and is light brown in color. U VI: Slightly consolidated, matrix-supported and poorly to moderately sorted gravel. The unit consists of two layers. The lower one is composed of gravel with a predominating matrix. Clasts are scarce, carbonated, centimeter-size, and subangular to subrounded. The matrix ranges from clay to silt and is light brown in color. The upper layer is made up of gravel with less matrix than the lower bed. Clasts are carbonated, subangular to subrounded, and range from a few centimeters to a few decimeters in size. The matrix ranges from silt to sand and is pink in color. Consolidation increases towards the top. V: Matrix-supported gravel lacking internal architecture. Clasts are carbonated, subrounded to rounded, and range from a few centimeters to a few decimeters in size. They are more abundant near the fault. The matrix ranges from clay to sand. Tz: Unconsolidated clays, dark brown in color containing scarce carbonated, centimeter-size clasts. This unit corresponds to a recent fluvial terrace.

Figura 16. Secciones de la trinchera 5, cuyas unidades forman parte de G3. Las líneas verdes gruesas indican calcretas y las rojas, fallas. Leyenda: T 1: Conglomerados soportados por la matriz, fuertemente cementados. Los clastos son carbonáticos, pobremente seleccionados, de subredondeados a redondeados y de dimensiones centimétricas a decimétricas. La matriz, de arcillosa a arenosa, es de color rosado. Hay abundantes costras de caliche laminar y oolítico en el interior de la unidad. Caliche oolítico a techo. T III: Conglomerados soportados por la matriz, bien cementados. Los clastos son carbonáticos, de dimensiones centimétricas, y presentan una selección de moderada a buena. La matriz, de arcillosa a arenosa, presenta un color marrón claro. U V: Gravas soportadas por la matriz, bien seleccionadas, no consolidadas. Los clastos son carbonáticos, subredondeados, de dimensiones centimétricas, ocasionalmente decimétricas. La cantidad de clastos disminuye hacia el techo. La localización preferente de los clastos define laminación interna. La matriz, de arcillosa a limosa, es de color marrón claro. U VI: Gravas soportadas por la matriz, de pobre a moderadamente seleccionadas, ligeramente consolidadas. La unidad consiste en dos capas. La inferior está formada por gravas con predominio de la matriz. Los clastos son escasos, carbonáticos, de dimensiones centimétricas, y de subangulosos a subredondeados. La matriz, de arcillosa a limosa, es de color marrón claro. La capa superior está formada por gravas con menos matriz que la capa inferior. Los clastos son carbonáticos, de subangulosos a subredondeados, y sus dimensiones de centimétricas a decimétricas. La matriz, de limosa a arenosa, es de color rosa. La consolidación aumenta hacia el techo. V: Gravas soportadas por la matriz, sin arquitectura interna. Los clastos son carbonáticos, de subredondeados a redondeados, y sus dimensiones de centimétricas a decimétricas. Són más abundantes junto a la falla. La matriz varía de arcillosa a limosa. Tz: Arcillas no consolidadas, de color marrón oscuro con escasos clastos carbonáticos de dimensiones centimétricas. Esta unidad corresponde a una terraza fluvial reciente.

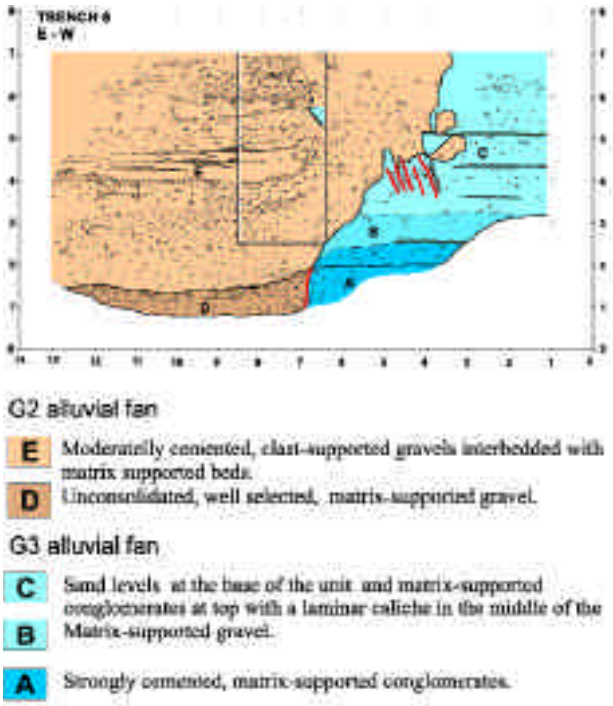

Figure 17. Log of trench 6. Thick red lines denote faults. Thick green lines indicate calcrete soils. White rectangle represents a portion of the trench that was more deeply dug. Legend: A: Strongly cemented, matrix-supported conglomerates. Clasts are limestone, sandstone and granite. They are subrounded to subangular, range from a few centimeters to a few decimeters in size, and are poorly sorted. Discontinuous laminar caliche on top. The matrix ranges from clay to sand and is pink in color. B: Matrix-supported gravel with a predominating matrix. The matrix ranges from clay to silt and is light brown in color. Clasts are scarce, mainly carbonated, centimeter-size, and subrounded to subangular. C: Well consolidated unit. From base to top: 1) sandstone with few pebbles containing conglomeratic channel fills composed of carbonated, centimeter-size, subangular clasts. 2) Laminar caliche. 3) Matrix supported conglomerates. Clasts are carbonated, range from a few centimeters to a few decimeters in size (reaching 40 cm in the upper part), and are poorly sorted. The matrix ranges from clay to silt and is pink in color. D: Clast-supported conglomerates. Clasts are carbonated, subrounded and moderately sorted. They are organized in a coarsening upwards sequence. The matrix ranges from clay to sand and is dark brown in color. E: Conglomeratic unit composed of matrix-supported beds and well sorted clast-supported conglomerates. The matrix ranges from clay to silt and is dark brown in color. Clasts are limestone, sandstone and granite. They are subangular to subrounded and centimeter-size. The unit contains channels of red clays containing few clasts and channels of clast-supported conglomerates.

Figura 17. Sección de la trinchera 6. Las líneas rojas gruesas indican fallas. Las líneas verdes gruesas representan calcretas. El rectángulo indica una parte de la trinchera que fué excavada más profundamente. Leyenda: A: Conglomerados soportados por la matriz, fuertemente cementados. Los clastos están formados por calizas, areniscas y granitos. Son de subredondeados a subangulosos, están pobremente seleccionados y sus dimensiones de centimétricas a decimétricas. Caliche laminar discontínuo a techo. La matriz, de arcillosa a arenosa, es de color rosa. B: Gravas soportadas por la matriz, con predominio de la matriz. La matriz, de arcillosa a limosa, es de color marrón claro. Los clastos son escasos, principalmente carbonáticos, de tamaño centimétrico, y de subredondeados a subangulosos. C: Unidad bien consolidada. De la base a techo: 1) arenisca con algunos cantos que contiene canales rellenos por conglomerados compuestos de clastos carbonáticos, tamaño centimétrico y subangulosos. 2) Caliche laminar. 3) Conglomerados soportados por la matriz. Los clastos son carbonáticos, sus dimensiones de centimétricas a decimétricas (alcanzan 40 cm en la parte superior), y están pobremente seleccionados. La matriz, de arcillosa a limosa, es de color rosa. D: Conglomerados soportados por los clastos. Los clastos son carbonáticos, subredondeados y moderadamente seleccionados. Están organizados en una secuencia granocreciente. La matriz, de arcillosa a arenosa, es de color marrón oscuro. E: Unidad conglomerática formada por capas soportadas por la matriz y por conglomerados soportados por los clastos. La matriz, de arcillosa a limosa, es de color marrón oscuro. Los clastos están formados por calizas, areniscas y granitos. Son de subangulosos a subredondeados y de tamaño centimétrico. Esta unidad contiene canales de arcillas rojas con algunos pocos clastos y canales de conglomerados soportados por los clastos.

completely modified and thus of no value to trenching. Therefore, the scarp between the site of trenches 1 and 2 and the northern limit of the segment at Porquerola creek was explored. Micro-topographic profiling and mapping together with field work and analysis of aerial photographs resulted in the selection of the Ermot site for trench 4. At this site recent deposits have accumulated in a locally depressed area adjacent to the scarp, which shows a smooth (rounded) profile. Trench 4 was dug across the scarp at a bend where it is slightly eroded by a small gully (Fig. 13). At this point the scarp is 6.5 m high. Trench 4 is up to 31 m long and 6 m deep, with an ESE-WNW orientation.

Trench analysis

The footwall is composed of a series of cemented conglomerates of alluvial origin, the uppermost unit of which is unit O. This is eroded close to the fault (Fig. 14). The hanging wall shows, at its base, the top of unit O capped by a well developed calcrete soil. Units Q and S - loose matrix supported gravels- overlie this cemented base level. In contrast, unit P, which has a wedge shape, is located adjacent to the main fault, and is composed of angular blocks of limestone conglomerates derived from unit O: it was interpreted as a colluvial wedge associated with a degraded fault scarp (Fig. 15). The trench shows two main faults (F1 and F2), which merge in depth, and

several small fractures and open cracks. F1 dips towards the east whereas F2 dips towards the west.

This trench revealed two paleoearthquakes: event X and event Y. The base of the colluvial wedge defines event horizon X. The vertical slip attributed to this event, 140 cm, is a minimum because it was obtained from the thickness of the colluvial wedge. According to McCalpin (1996), the maximum thickness of a scarp colluvium is limited to half the height of the free face from which it was removed. The western part of this colluvial wedge and the base of unit Q1 were faulted again by a younger event along F2 (event Y). The scarp formed during this last event is buried by the upper part of unit Q1 on the southern wall.

Although the calcrete soil on top of unit O was sampled for absolute dating, the samples were all highly contaminated. Given its regional position, i.e. over the G3 alluvial fans, the development of this soil can be attributed, with little uncertainty, to the phase of calcrete formation, 125 ka ago. Pollen analysis of units Q and S revealed that the latter is Holocene in age (P28, P29, table 1). Therefore, events X and Y occurred in the time interval between 125 ka BP and the Holocene. Event X in trench 4 chronologically overlaps event X in trenches 1 and 2 with the result that these events can be correlated. In contrast, event Y cannot be correlated with the other events described since it took place after event X but before the Holocene, whereas event Z in trenches 1, 2 and 3 occurred in the late Holocene.

Trenches 5 and 6

These two trenches were planned to better constrain the limits of the two segments of the El Camp fault. Mapping indicated a difference in behavior between the area near Montroig, where the fault was sealed by the upper part of the G3 deposits, and the southern part of the scarp, where the G3 deposits were cut by the fault. However, the location of the limit was not clear, which could result in an over- or underestimation of the length of surface rupture by several kilometers. The two selected sites were the Porquerola and Rifà creeks (trenches 5 and 6 respectively).

Trench 5 was dug along the northern bank of Porquerola creek where the fault crops out across the creek bed and coincides with a 4 m high morphological scarp which cannot be associated with a fault scarp owing to the modification of the land in the area. The site is located on the G3 alluvial fan deposits. The trench consisted of two walls at different topographic levels of the northern river bank (Fig. 16). Both walls revealed two faults, F1 and F2, the latter being more developed in the upper trench. Fault F2 reaches the surface in this trench, thereby confirming the view that the morphological scarp is a fault scarp. Since the fault cuts the G3 alluvial fan up to the surface, the boundary between the northern and the southern segments should be located to the North of Porquerola creek.

The northern bank of Rifà creek showed, before trenching, an incomplete outcrop of the El Camp fault. The fault separated the cemented conglomerates of the G2 alluvial fans in the footwall from the less cemented conglomerates of the G3 alluvial fans in the hanging wall. Trench 6 was only dug to determine the upward limit of the fault (Fig. 17). The trench revealed that the upper G3 sediments had sealed the fault at this site with the result that the activity of the fault at this site ceased during the deposition of this unit, i.e. between 300 and 125 ka BP. This suggests that the segment boundary is situated between the Porquerola and Rifà creeks.

Trench 7

The southernmost fault scarp, which is associated with the El Camp fault, is situated in the Almadrava area (Fig. 3). Despite the fact that the conditions of this part of the scarp are not suitable for trenching (highly modified area), its strategic position at the end of the onshore part of the fault renders it valuable. The investigation consisted in the re-interpretation (Masana, 1996) of a wall of an abandoned trench which was dug mainly on the uplifted wall of the fault but also, to a lesser extent, across the fault. The trench (Fig. 18) is 27 m long, oriented E-W

Table 2. Vertical displacement per event observed at different trenches.

Tabla 2. Desplazamiento vertical por evento observado en las diferentes trincheras.

	Event Z	Event Y	Event X
TR1	40-100 cm		140-200 cm
TR2	70 cm		
TR3	>30 cm		
TR4		40 cm	140 cm

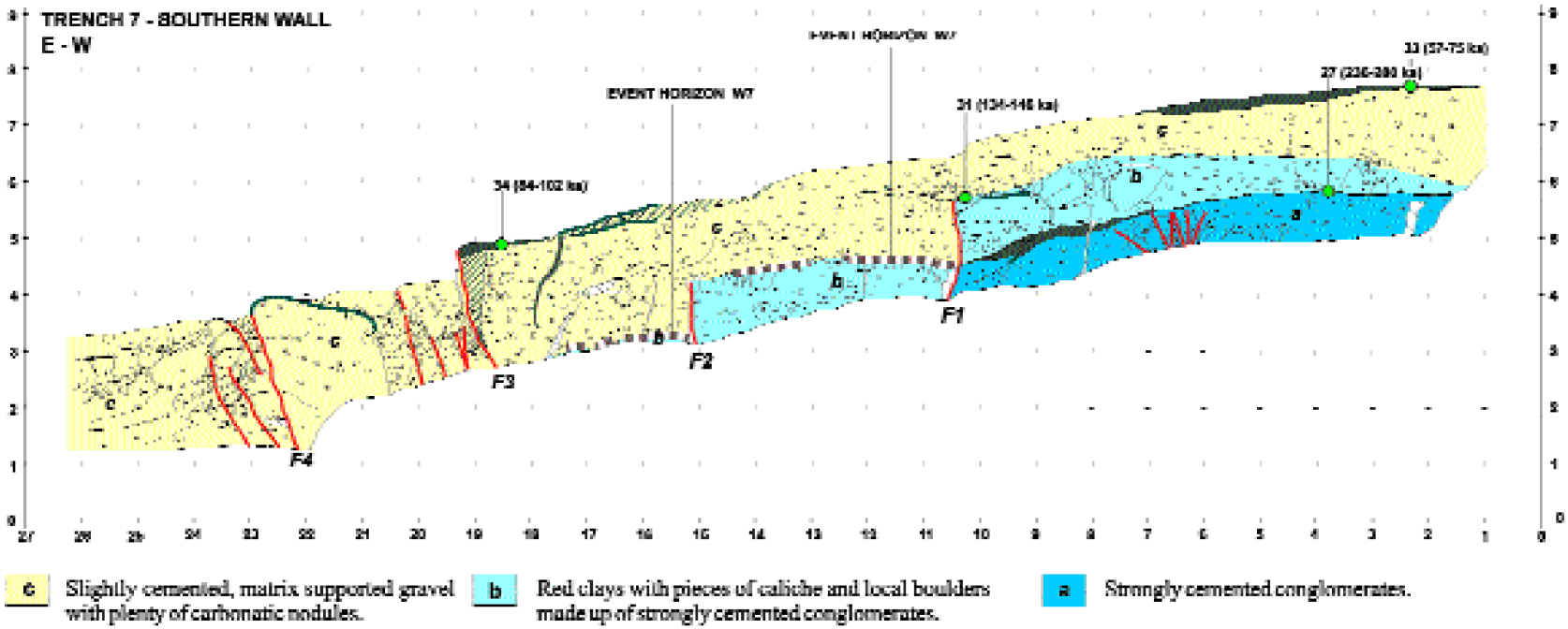

Figure 18. Log of trench 7. Colored circles indicate samples for dating (green: TL). Thick red lines represent faults. Thick green lines indicate calcrete soils. Legend: a: Strongly cemented, matrix-supported (locally clast-supported) conglomerates. Clasts are carbonated, heterometric (from 0.5 to 20 cm), and angular. Laminar and oolitic caliche on top. b: Red clays with pieces of caliche and carbonated nodules. Locally, this unit contains boulders of up to 1.5 m in diameter of strongly cemented conglomerates composed of heterometric carbonated clasts. Caliche crusts in the upper part of the unit. c: Moderately cemented, matrix-supported gravel. Clasts are carbonated, 3 to 5 cm in size, and subangular. There are plenty of carbonated nodules. Caliche crusts are well developed on the top and along the joints.

Figura 18. Sección de la trinchera 7. Los círculos coloreados indican muestras para dataciones (verde: TL). Las líneas rojas gruesas representan fallas. Las líneas verdes gruesas indican calcretas. Leyenda: a: Conglomerados soportados por la matriz (localmente soportados por los clastos), fuertemente cementados. Los clastos son carbonáticos, heterométricos (de 0,5 a 20 cm) y angulosos. Caliche laminar y oolítico a techo. b: Arcillas rojas con fragmentos de caliche y nódulos carbonáticos. Localmente esta unidad contiene bloques de hasta 1,5 m de diámetro de conglomerados fuertemente cementados formados por clastos carbonáticos heterométricos. Costras de caliche en la parte alta de la unidad. c: Gravas soportadas por la matriz, moderadamente cementadas. Los clastos son carbonáticos, de 3 a 5 cm, subangulosos. Hay abundantes nódulos carbonáticos. A techo y a lo largo de las diaclasas hay costras de caliche bien desarrolladas.

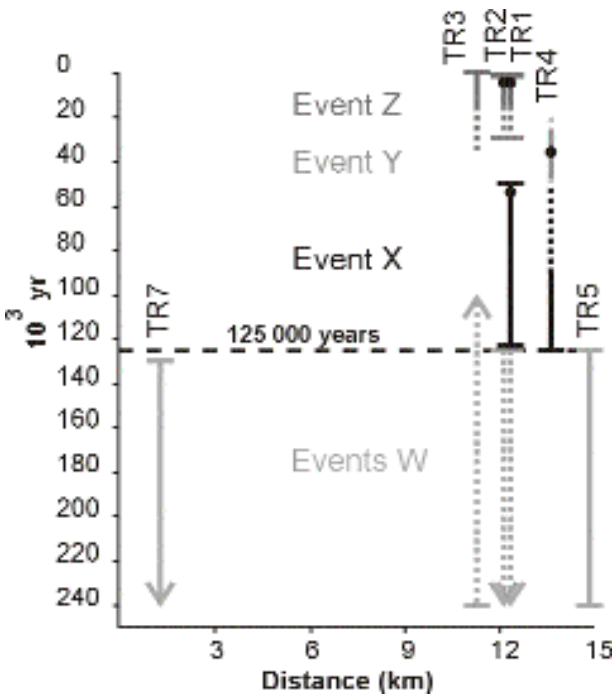

Figure 19. Sketch indicating the time constraints of the events revealed by trench analysis. Dotted lines indicate poorly constrained chronological information. Black dots show the most plausible chronological positions of the events. Lines labeled W were not attributed to single events but correspond to cumulative displacements.

Figura 19. Esquema que sintetiza los datos temporales referentes a los eventos puestos de manifiesto mediante el análisis de las trincheras. La línea discontínua indica información pobremente definida. Los puntos negros muestran las posiciones cronológicas más plausibles de los eventos descritos. Las líneas indicadas con W no representan eventos individuales, sino desplazamientos acumulados.

and dug into an alluvial fan forming part of the G3 generation. It exposes four main faults, the best developed being F4. The position of F4 coincides with the base of the fault scarp, which at this site shows a 9 m vertical offset in accordance with microtopographic profiling.

The oldest sediments (unit a) outcropping in trench 4 are composed of highly cemented conglomerates with calcrete on top, yielding an age of 300 ka BP using TL. Thus, unit a forms part of the G2 fans. Units b and c are loose conglomerates containing a number of carbonated soils. TL dating (table 1) indicates that the calcrete on top of unit c can be attributed to the widespread phase of calcrete development 125 ka ago. F1 and F2 cut the top of unit b with a vertical displacement of 1.3 m. It is not possible to determine whether this displacement is due to one or more events, but there is no doubt that it took place after 300 ka BP and before 125 ka BP. F3 and F4 displaced unit c and the calcrete soil developed on top of it. Hence, these faults slipped after 125 ka BP. Although the poor age constraints of these events do not allow a correlation with the other trenches, they indicate that the fault was active in this part of the scarp after 125,000 yr with the result that this sector forms part of the southern segment of the El Camp fault.

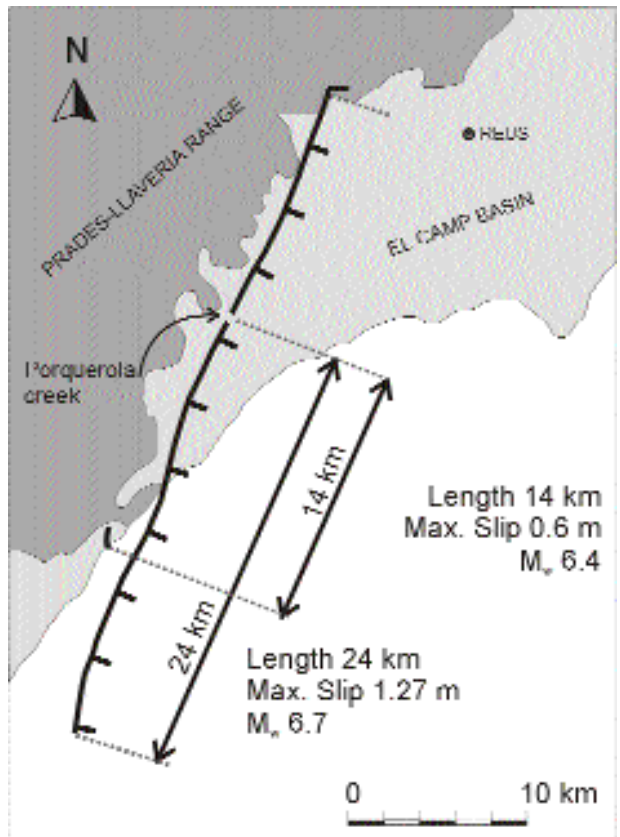

Figure 20. General map of the El Camp fault area showing the limits of the two segments. The length of the southern and active segment may vary between 14 and 24 km depending on whether the offshore part is considered or not. Maximum slip per event and M_W are attributed to the two possible cases in accordance with the regression lines of Wells and Coppersmith (1994).

Figura 20. Mapa general del área de la falla de El Camp con indicación de los dos segmentos. La longitud del segmento meridional y activo puede variar entre 14 y 24 km dependiendo de si se considera la parte submarina de la falla o no. Se asigna el máximo salto por evento y la M_W a cada uno de los casos de acuerdo con las líneas de regresión de Wells y Coppersmith (1994).

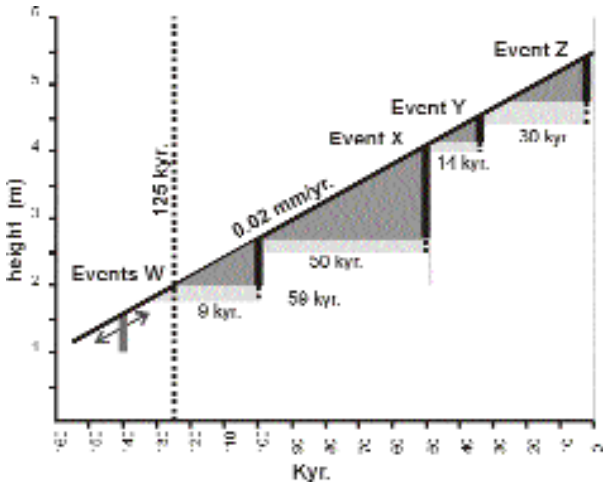

Figure 21. Sketch of the paleoseismic data obtained in this study. Black vertical bars represent the detected seismic events located at their best chronological estimate. Their length indicates the vertical displacement with error bars shown as dotted lines. Event X is divided into two possible events, the youngest of which has a constrained vertical displacement. Deformation predating 125 ka BP is represented by a vertical gray bar with an arbitrary position on the time axis. Duration of inter-seismic periods is also indicated.

Figura 21. Esquema con los datos paleosísmicos obtenidos en este estudio. Las barras negras verticales representan los eventos sísmicos detectados, situados en su mejor estimación cronológica. Su longitud indica el desplazamiento vertical con el error indicado en línea discontínua. El evento X se ha dividido en dos posibles eventos, el más reciente de los cuales tiene un desplazamiento vertical bien definido. La deformación previa a 125 ka BP se ha representado con una barra gris vertical en una posición arbitraria en el eje del tiempo. También se ha indicado la duración del período intersísmico.

Summary of paleoseismic events and related displacements

Trench analysis revealed a number of well constrained events postdating the 125 ka old surface (events Z, Y and X) as well as several poorly-constrained deformation structures predating this surface (events W) (Fig. 19).

The most recent event, event Z, was clearly evidenced by colluvial wedges on all the walls of trenches 1 and 2 and was also identified in trench 3. It took place between 1195 yr AD and 31,490 yr BP although it most probably occurred around 3000 yr BP, just before the age of the bottom of the colluvial wedge. The vertical slip (table 2) was estimated to be between 0.4 and 1 m in trenches 1 and 2.

Event Y was identified owing to a fault which cuts a previously deposited colluvial wedge. This event was regarded as being distinct from the other two events (Z and X) since the geological record in trench 4 indicates that it took place prior to the Holocene (the most probable time for event Z) and after an event that was correlated with event X. Therefore, the chronological constraints for event Y depends on the age of the other events. The vertical slip (table 2) was estimated to be 0.4 m.

Evidence for event X was found in trenches 1 and 4 in the form of a buried fault scarp and a colluvial wedge, respectively. In both cases, the record indicates that the earthquake occurred later than 125 ka BP. In trench 1 it took place before the deposition of unit C (unit D, overlying C, yielded an age of 31 ka BP) and after the formation of the calcrete soil which gave an age of 125 ka BP. In trench 4, the event occurred after the 125 ka old calcrete soil and before event Y. The restoration of the vertical deformation along the southern wall of trench 1 (Fig. 11) shows that the vertical offset attributed to the last event (event Z, 40-100 cm) is only half that ascribed to event X (140-200 cm). This suggests that the vertical deformation attributed to event X could have been produced by two events instead of only one. Nevertheless, the thickness of the colluvial wedge in trench 4 is 1.4 m, which must be considered to be the minimum of the vertical offset during one of these possible events. Therefore, if two events are interpreted, they should be different in size: 1.4 and 0.6 m each.

DISCUSSION

The El Camp fault is a normal fault. Regional surface data (Núñez et al., 1980) and subsurface data (wells and seismic profiling, Sàbat et al., 1997) show that it is an eastward dipping fault whose eastern wall has subsided since the early Miocene. Despite this, in trenches 3, 4 and 7, some of the small faults, making up the El Camp fault, dip steeply to the WNW, displaying a reverse fault attitude. This should correspond to a local effect, e.g. reverse secondary faults related to extensional forced folding caused by a steep normal fault at depth.

Detailed mapping of the fault scarp and regional alluvial fans, together with trenching analysis, revealed a different behavior in the northern and the southern parts of the fault (Fig. 20), resulting in the recognition of two segments along the El Camp fault: to the North of Porquerola creek the fault became inactive between 300 and 125 ka BP; to the South it continues to be active (Fig.

20). The northern segment is 16 km long and the southern segment is 24 km long (14 km long onshore and at least 10 km offshore according to seismic reflection data from the continental shelf, Medialdea et al., 1986). The discussion below will focus on this active segment.

Micro-topographic profiles perpendicular to the fault scarp were used to determine the vertical dislocation undergone by the regionally extensive 125 ka old calcrete soil. The vertical dislocation of this surface was variable (from 3 to 9 m) and therefore different values of slip rate were obtained at different trench sites. In trench 3 the depositional wedge shape of unit J (Fig. 12) indicates that it developed at the foot of a preexisting scarp. This suggests that the 125 ka surface already displayed a scarp. Therefore, the slip rates obtained are probably overestimates and thus the lowest value (0.02 mm/yr) is probably the one closest to reality.

Considering the uncertainties in the chronological constraints of the events, an estimate of the average recurrence period can be made with the available data plotted in Fig. 21. If one or two events, varying in size, were considered for event X, the average inter-seismic period (considering 125 ka) would range between 42 and 25 ka (for the latter we consider that an earthquake that predates event X occurred a short time prior to 125 ka). This would be consistent with the values obtained if a slip per event between 1 m and 0.7 m were taken into account to produce a cumulative vertical dislocation of 3.5 m in 125 ka: these results would range between 25 and 36 ka. Hence, the mean recurrence period would be between 42 and 25 ka but probably closer to 30 ka.

Given that the most recent earthquake, event Z, occurred shortly before the deposition of the colluvial wedge in trenches 1 and 2, the elapsed time barely exceeds 805 yr and is probably around 3000 yr. This means that the seismic cycle along the El Camp fault has recently restarted, diminishing the seismic hazard (time-dependent model for seismic hazard calculation).

The maximum expected earthquake along this fault was estimated by comparing the vertical slip per event observed in the trenches and the total length of the rupture with the same parameters observed in historical earthquakes of known magnitude produced by normal faults (Wells and Coppersmith, 1994). The maximum slip for a single event observed in the trenches is 1.4 m (in trenches 1 and 4, see table 2), which implies a M_W of 6.7+/-0.1. The length of the rupture may vary between 14 km and 24 km, depending on whether the offshore part of the fault is considered or not. This corresponds to a M_W of 6.4+/-0.4 for the former, and a M_W of 6.7+/-0.5 for the latter. Although the offshore part of the fault warrants further study to better characterize its geometry and seismic behavior, the magnitude obtained (considering a total length of 24 km for the fault segment) is consistent with that obtained using the vertical slip.

ACKNOWLEDGMENTS

This study was co-funded by the Consejo de Seguridad Nuclear (CSN) and the Empresa Nacional de Residuos Radioactivos (ENRESA) with the contribution of the Vandellós II Nuclear power plant (Datación project). During the development of the project we benefited from discussions with J.G. Sánchez Cabañero (CSN) and J. Plaza (ENRESA). Thermoluminiscence dating was done at the Universidad Autónoma de Madrid, U/Th and pollen analysis at the Institut Jaume Almera de Ciències de la Terra (CSIC), and Radiocarbon dating at Beta Analytics Inc. We thank R. Julià, F. Burjachs, M. Garcés, T. Calderón, P. Beneitez and A. Millán for their helpful discussions and contributions on dating. The reviews by M. Meghraoui and Ch. Vaneste greatly helped to improve the manuscript. We also thank M. López Gilabert (Urbanización Bonmont Terres Noves S.A.), M. S. Mendoza, and J. Puig Castelló for permission to trench on their properties.

REFERENCES

Anadón, P., Cabrera, L., Calvet, F., Gallart, F., López, C., Permanyer, A., Serra-Kiel, J., 1983. El Terciario. In I.G.M.E. (ed.), Estudio geológico del Maestrazgo y de la mitad meridional de los Catalánides, 1-179.

Banda, E., Santanach, P., 1992. The Valencia trough (western Mediterranean): an overview. Tectonophysics, 208, 183-202.

Camelbeeck, T., Meghraoui, M., 1998. Geological and geophysical evidence for large paleoearthquakes with surface faulting in the Roer Graben (northwest Europe). Geophys. J. Int., 132, 347-362.

Fontboté, J.M., Guimerà, J., Roca, E., Sàbat, F., Santanach, P., Fernández-Ortigosa, F., 1990. The Cenozoic Geodynamic evolution of the València trough (western Mediterranean). Rev. Soc. Geol. España, 3(3-4), 249-259.

Giardini, D., 1995. The geological input in the practice of seismic hazard assessment: the Kobe lessons. In L. Valensise, D. Pantosti (eds.), International school of solid earth geophysics, 11th course: Active faulting studies for seismic hazard assessment, Erice-Sicily: Istituto Nazionale di Geofisica.

Lanaja, J.M., 1987. Contribución de la exploración petrolífera al conocimiento de la geología de España. Instituto Geológico y Minero de España, 465 p.

Machette, M.N., Personious, S.F., Nelson, A.R., 1992. Paleoseismology of the Wasatch fault zone: A summary of recent investigations, interpretations, and conclusions. In P.L. Gori, Hays, W.W. (eds.), Assessment of Regional Earthquake Hazards and Risk Along the Wasatch Front, Utah, U.S. Geol. Surv. Prof. Pap., 1500-A, A1-A71.

Masana, E., 1995. L'activitat neotectònica a les Cadenes Costaneres Catalanes. Tesi doctoral, Universitat de Barcelona, 444 p.

Masana, E., 1996. Evidence for past earthquakes in an area of low historical seismicity: the Catalan coastal ranges, NE Spain. Annali di Geofisica, 39, 689-704.

Mauffret, A., Fail, J.P., Montadert, L., Sancho, J., Winnock, E., 1973. Northwestern Mediterranean sedimentary basin from seismic reflection profile. Amer. Assoc. Petrol. Geol. Bull., 57, 2245-2262.

McCalpin, J. (ed.), 1996. Paleoseismology. San Diego, Academic Press cop., 588 p.

Medialdea, J., Maldonado, A., Alonso, B., Díaz, J.I., Farrán, M., Giró, S., Vázquez, A., Sainz-Amor, E., Martínez, A., Medialdea, T., 1986. Mapa geológico de la plataforma continental española y zonas adyacentes, escala 1:200.000, hoja 41-42, Tortosa-Tarragona, mem. expl., 78 p., Madrid, IGME, Centro de Publicaciones Ministerio de Industria y Energía.

Núñez, A., Colodrón, I., Ruiz, V., Cabañas, I., Uralde, A., Abellán, F. et al., 1980. Mapa geológico de España, escala 1:50.000. Primera edición, hoja 472, Madrid, I.G.M.E.

Roca, E., Guimerà, J., 1992. The Neogene structure of the eastern Iberian margin: structural constraints on the crustal evolution of the València trough (Western Mediterranean). Tectonophysics, 203, 203-218.

Sàbat, F., Roca, E., Muñoz, J.A., Vergés, J., Sans, M., Masana, E., Santanach, P., Estévez, A., Santisteban, C., 1997. Role of extension and compression in the evolution of the eastern margin of Iberia: the ESCI-Valencia Trough seismic profile. Rev. Soc. Geol. España, 8(4), (1995), 431-448.

Sieh, K., 1978. Prehistoric large earthquakes produced by slip on the San Andreas fault at Pallet Creek, California. J. Geophys. Res., 83, 3907-3939.

Suriñach, E., Roca, A., 1982. La sismicidad en la zona comprendida entre 40N-44N y 3W-5E. NE Península Ibérica. In A. Roca, E. Suriñach (eds.), Catálogo de terremotos de Cataluña, Pirineos y zonas adyacentes. Publicación de la cátedra de geofisica, Universidad Complutense de Madrid, 9-106.

Villamarín, J.A., Masana, E., Calderón, T., Julià, R., Santanach, P., 1999. Abanicos aluviales cuaternarios del Baix Camp (provincia de Tarragona): resultados de dataciones radiométricas. Geogaceta, 25, 211-214.

Wells, D.L., Coppersmith, K.J., 1994. New empirical relationships among magnitude, rupture length, rupture area and surface displacement. Bull. Seism. Soc. Am., 84, 974-1002.